Wen *et al. Energy Mater* 2024;4:400054
DOI: 10.20517/energymater.2024.08

Energy Materials

Review

Open Access

Check for updates

Recent advances of cobalt-free and nickel-rich cathode materials for lithium-ion batteries

Lang Wen[1,3], Fang Cheng[2,3,*], Xiaoqu Wang[1,3], Xinyu Zeng[1,3], Ting Wang[1,3,4], Litao Li[1,3,4], Yuqin Hu[1,3], Qiang Yu[2,3,4], Wen Lu[1,2,3,4,*]

[1]School of Materials and Energy, Yunnan University, Kunming 650091, Yunnan, China.
[2]College of Chemical Science and Engineering, Yunnan University, Kunming 650091, Yunnan, China.
[3]Institute of Energy Storage Technologies, Yunnan University, Kunming 650091, Yunnan, China.
[4]Southwest United Graduate School, Kunming 650092, Yunnan, China.

***Correspondence to:** Prof./Dr. Wen Lu, Institute of Energy Storage Technologies, Yunnan University, 182 Street 121, Kunming 650091, Yunnan, China. E-mail: wenlu@ynu.edu.cn; Prof./Dr. Fang Cheng, College of Chemical Science and Engineering, Yunnan University, Kunming 650091, Yunnan, China; Institute of Energy Storage Technologies, Yunnan University, Kunming 650091, Yunnan, China. E-mail: chengfang@ynu.edu.cn

How to cite this article: Wen L, Cheng F, Wang X, Zeng X, Wang T, Li L, Hu Y, Yu Q, Lu W. Recent advances of cobalt-free and nickel-rich cathode materials for lithium-ion batteries. *Energy Mater* 2024;4:400054. https://dx.doi.org/10.20517/energymater.2024.08

Received: 23 Jan 2024 **First Decision:** 2 Apr 2024 **Revised:** 25 Apr 2024 **Accepted:** 14 May 2024 **Published:** 31 May 2024

Academic Editor: Yuping Wu **Copy Editor:** Fangling Lan **Production Editor:** Fangling Lan

Abstract

In order to satisfy the rapidly increasing demands for a large variety of applications, there has been a strong desire for low-cost and high-energy lithium-ion batteries and thus for next-generation cathode materials having low cost yet high capacity. In this regard, the research of cobalt (Co)-free and nickel (Ni)-rich (CFNR) layered oxide cathode materials, able to meet the low-cost and high-capacity requirements, has been extensively pursued but remains challenging largely due to the elimination of Co and high content of Ni in these materials. Herein, we systematically review the challenges and recent advances of CFNR cathode materials on these important aspects. Specifically, we first clarify the role of Co in Ni-rich layered oxides and the possibility of its elimination to fabricate CFNR cathode materials. We then discuss the methods developed to synthesize these cathode materials. This is followed by the elucidation about their degradation mechanisms and the research progress of modification strategies achieved in enhancing the properties for these materials. Finally, we discuss the current challenges and future prospects of CFNR cathode materials as the next-generation cathode materials for low-cost and high-energy lithium-ion batteries.

Keywords: Lithium-ion batteries, cathode materials, cobalt-free, nickel-rich, layered oxides

INTRODUCTION

Since their first commercialization by Sony in 1991, lithium-ion batteries (LIBs) have been used for a large variety of applications, including portable electronic devices, electric vehicles, and renewable energy storage systems[1-4]. To satisfy the rapidly increasing demands for these applications, lowering the cost and enhancing the energy density have been two important tasks for LIBs[5]. These, in turn, continuously propelled the research and development of the cathode materials of LIBs because they are the core component accounting for more than half of the cost and largely determining the energy density of LIBs[5].

$LiCoO_2$ (LCO) was the cathode of Sony's LIBs in 1991 and has been predominantly employed in LIBs for 3C (Computer, Communication, Consumer) electronic devices[1,2]. However, owing to the inherently scarce resource of cobalt (Co) [Figure 1A] and the rapid expansion in production capacity of LIBs, the cost of Co continued to increase over the past decade [Figure 1B]. In conjunction with the environmental unfriendliness of Co, this indeed triggered a vigorous desire for lowering the Co content in cathode materials[1,3,4]. In this regard, by substituting the Co of LCO with other transition metals (TM), the resultant layered oxides, such as lithium nickel cobalt manganese oxide ($LiNi_xCo_yMn_zO_2$) and lithium nickel cobalt aluminum oxide ($LiNi_xCo_yAl_zO_2$), have shown their great opportunity in lowering Co content and have become an important family of cathode materials for LIBs[1,3,4].

It is known that nickel (Ni) is the key element that determines the capacity and energy density of layered oxides[3,5], with $LiNiO_2$ (LNO) possessing a high theoretical specific energy density of ~1,050 Wh kg^{-1}[6]. Thus, along with the aforementioned consideration of lowering the cost of LIBs, the percentage of Ni has been increased and that of Co decreased in layered oxides to realize lower cost and higher energy density for LIBs[1,3,5]. As shown in Figure 1C, the energy density enhancement of $LiNi_xCo_yMn_zO_2$ upon the simultaneous increase and decrease of its Ni and Co contents, respectively, represents a good example of such kind (with respect to LCO)[1,3,4]. Moreover, the complete elimination of Co while further increasing the Ni content, resulting in the so-called Co-free and Ni-rich (CFNR) layered oxides as the next-generation cathode materials, has been considerably investigated in recent years to meet the ultimate goal of low-cost and high-energy LIBs[7-11]. In this sense, for example, extensive studies demonstrated that $LiNi_xM_{1-x}O_2$ ($x \geq 90\%$, M represents a metal other than Co) can achieve an ultrahigh specific capacity (≥ 200 mAh g^{-1}) and energy density (800 Wh kg^{-1}) with its cost estimated to be less than 20 $ kWh^{-1}[3,5,9,10,12-19].

Nevertheless, an immediate concern about the feasibility of the CFNR design can be logically put forward, which is associated with a prevailing belief about the essentiality of Co[1,20] and the issues from a high Ni content (such as cation mixing[7,21], side reactions[15,21,22], and microcracking[9,13]) in layered oxide cathode materials. This has indeed spurred the extensive research of CFNR cathode materials in recent years, and with their achievements and issues reviewed but sporadically[1-4]. In this paper, therefore, we systematically and comprehensively review the aspects, covering the essentiality of Co, synthesis methods, degradation mechanisms, and modification strategies, of CFNR cathode materials. Specifically, we begin our discussion about clarifying the role of Co in and the possibility of its elimination from the Ni-rich layered oxides. This is followed by a discussion about the synthesis methods, the degradation mechanisms, and the research progress of modification strategies achieved in enhancing the properties of CFNR cathode materials. Finally, the current challenges and future prospects of these materials are summarized, which would encourage more research and development on them as the next-generation cathode materials for low-cost and high-energy LIBs.

THE ROLE OF COBALT IN NICKEL-RICH CATHODE MATERIALS

Largely owing to its advantages of good electronic conduction and low Li/Ni mixing, Co is considered an

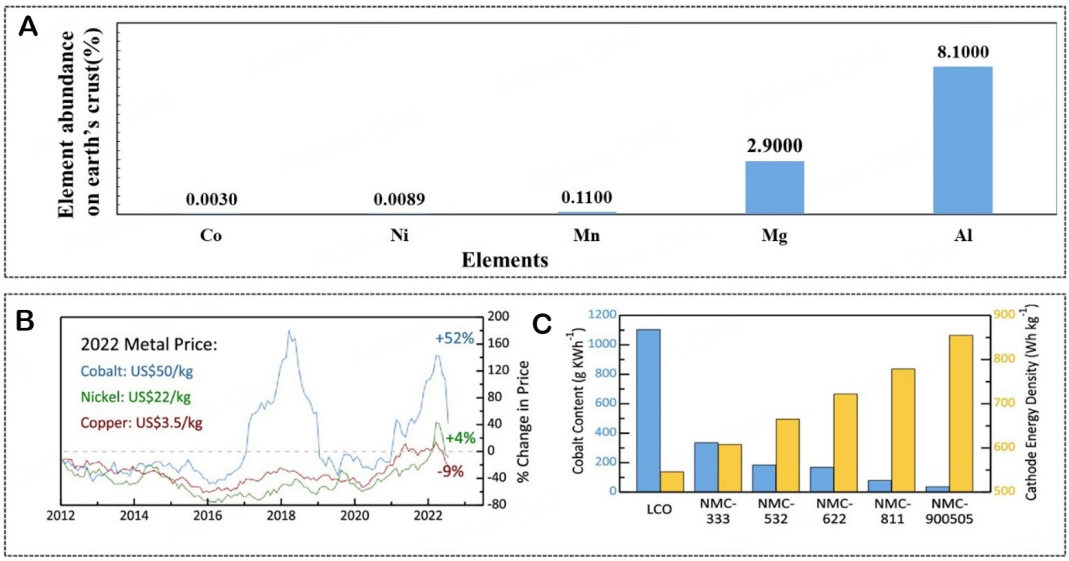

Figure 1. (A) Abundances of cobalt, nickel, manganese, magnesium, and aluminum on the earth's crust. (B) Price chart of raw cobalt, nickel, and copper in the past decade (2012 to August 2022), (C) Energy density and cobalt content of typical layered oxides, ranging from $LiCoO_2$ (LCO) to $LiNi_xMn_yCo_zO_2$ (NMC-xyz) of increasing nickel content. This figure is quoted with permission from Lee *et al.*[1].

essential element for Ni-rich layered oxides, such as the widely used commercial cathode materials of $LiNi_{0.8}Co_{0.1}Mn_{0.1}O_2$ (NCM811) and $LiNi_{0.8}Co_{0.15}Al_{0.05}O_2$ (NCA81505)[20,23,24]. It has been believed that Co^{3+} is essential for charge balancing to alleviate the negative effect of Mn^{4+} in producing Ni^{2+}[1]. Also, Co^{3+} does not have a magnetic moment and can help relieve the magnetic frustration caused by Ni^{2+}[2]. Both can inhibit Li/Ni mixing and thereby ensure a well-crystallized and stable structure for layered oxides[25]. For example, Figure 2A shows the gradual increase of the formation energy of one pair Li/Ni exchange (and hence the suppression in Li/Ni mixing) due to the inhabited Ni^{2+}-O^{2-}-Co^{3+} superexchange interaction upon the Co content increase for a series of $Li(Ni_xMn_yCo_z)O_2$ (NMC) materials[26].

However, recent studies raised a question about the effectiveness and necessity of Co in Ni-rich layered oxides[1,2]. For example, when compared to magnesium (Mg), manganese (Mn), and aluminum (Al), the 5% substitution of Co was found ineffective in suppressing the multiphase transition during the electrochemical process of LNO [Figure 2B][2,3,27]. Also, as shown in Figure 2C, upon delithiation (charge), the Ni-rich $LiNi_{0.6}Co_{0.4}O_2$ (NC64) encountered a change of > 5% in the c-axis lattice parameter, and such a considerable structural expansion and contraction can potentially lead to particle damage and hence intragranular microcracking in NC64. Interestingly, this issue of NC64 was significantly alleviated when Co was gradually replaced with Mn, resulting in reduced lattice parameter changes for $LiNi_{0.6}Mn_{0.2}Co_{0.2}O_2$ (NMC622) and $LiNi_{0.6}Mn_{0.4}O_2$ (NM64) [Figure 2C][28]. Here, while Co inevitably exacerbates the phase transformation and hence induces a rapid structural degradation, the suppression of such kind by Mn has been demonstrated to be due to its optimized Li/Ni disorder building a "bearing beam" to stabilize the layered structure of the Mn-containing Ni-rich materials[28]. These studies suggest the unnecessity of Co and, instead, the capabilities of alternative dopants such as Mg, Mn, and Al in providing sufficient structural stability and well-defined electrochemical performance for Ni-rich layered oxides, which, therefore, indicates the feasibility of CFNR layered oxides as the next-generation cathode materials for low-cost and high-energy LIBs[1,2,29-31].

SYNTHESIS OF CFNR CATHODE MATERIALS

Broadly, as for conventional layered oxides, CFNR cathode materials can be synthesized in either a solid or

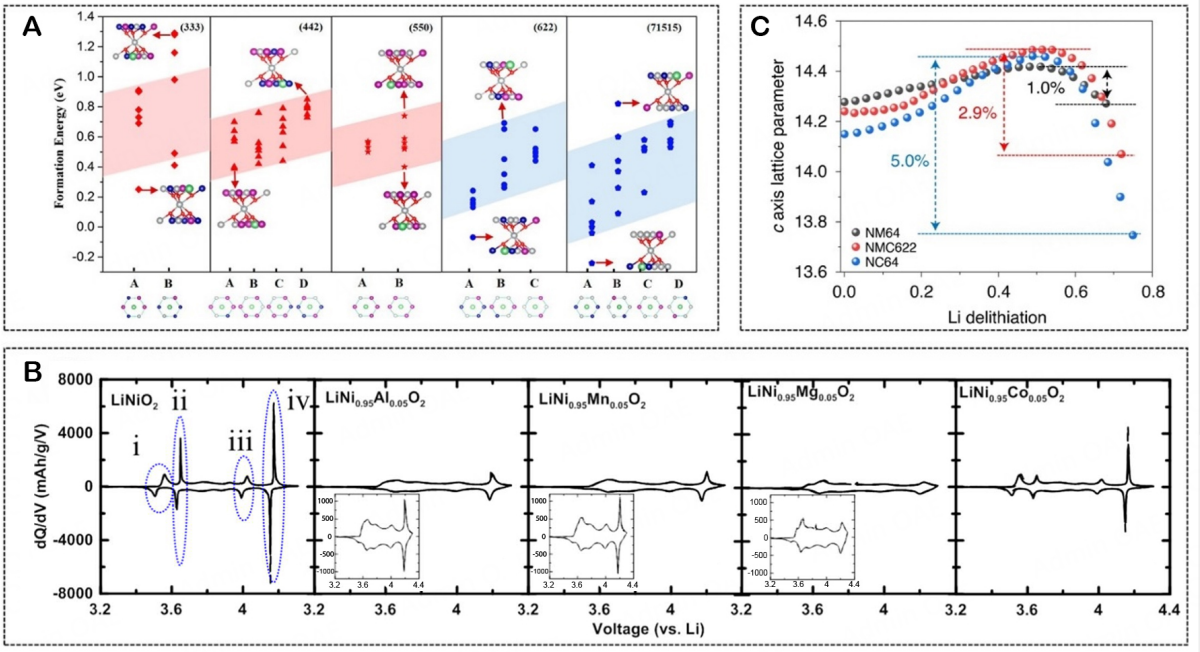

Figure 2. (A) Formation energy (E_f) of one pair of Ni/Li exchange in $LiNi_{1/3}Mn_{1/3}Co_{1/3}O_2$ (333), $LiNi_{0.4}Mn_{0.4}Co_{0.2}O_2$ (442), $LiNi_{0.5}Mn_{0.5}O_2$ (550), $LiNi_{0.6}Mn_{0.2}Co_{0.2}O_2$ (622), and $LiNi_{0.7}Mn_{0.15}Co_{0.15}O_2$ (71515) with zigzag TM arrangements. The local configurations of Ni/Li exchanges with the lowest and highest E_f are shown in each material. The shaded areas show the general trend of the E_f variation for the Ni/Li exchange, and the schematics at the bottom represent the nonequivalent ion environment for the antisite Li ion in the TM layer. This figure is quoted with permission from Zheng *et al.*[26]. (B) Differential capacity as a function of cell voltage (dQ/dV *vs.* V) of 2nd charge and discharge of $LiNiO_2$, $LiNi_{0.95}Al_{0.05}O_2$, $LiNi_{0.95}Mn_{0.05}O_2$, $LiNi_{0.95}Mg_{0.05}O_2$, and $LiNi_{0.95}Co_{0.05}O_2$. This figure is quoted with permission from Li *et al.*[27]. (C) The c-axis lattice parameter changes in the as-prepared samples obtained from Rietveld refinements. The lattice changes of the c axes of NC64 ($LiNi_{0.6}Co_{0.4}O_2$), NMC622 ($LiNi_{0.6}Mn_{0.2}Co_{0.2}O_2$) and NM64 ($LiNi_{0.6}Mn_{0.4}O_2$) were 5.0%, 2.9% and 1.0%, respectively. This figure is quoted with permission from Liu *et al.*[28].

wet state. In a typical solid-state reaction procedure, a CFNR cathode material is obtained by mixing its raw reactant materials first, followed by sintering the mixture thus prepared at a high temperature and in an oxygen atmosphere[32-35]. Using this process, for example, Croguennec *et al.* synthesized $LiNi_{1-x}Ti_xO_2$ by sintering its raw material mixture of Li_2O, NiO, and TiO_2 under an oxygen gas flow at 800-870 °C[35]. Usually, the solid-state reaction methods have the distinct advantage of ease of operation but the disadvantage of nonuniform elemental distribution and potential generation of impurity phases for the products. In this regard, CFNR cathode materials have been extensively researched (and even mass-produced) in a wet state. Particularly, in these methods, they are synthesized by preparing their precursors first, followed by calcinating the resultant precursors with a lithium source under the conditions of a high temperature and an oxygen atmosphere. Moreover[36-40], the precursors of the CFNR layered oxides can be obtained through various approaches, including electrolytic, sol-gel, hydrothermal, and co-precipitation methods.

Specifically, in a typical electrolytic method, two nickel metal plates are used as both the cathode and anode that are immersed in an aqueous electrolyte. Upon stirring the electrolyte, a current is applied to oxidize the anode to extract Ni ions into the electrolyte, which are transported towards the cathode under the electric field and the electrolyte stirring. At the cathode, the reduction of water generates hydroxide ions (and hydrogen gas) which interact with the Ni ions from the anode to form nickel hydroxide [$Ni(OH)_2$]. Using this approach[39], Ji *et al.* synthesized a LNO cathode by sintering the as-prepared $Ni(OH)_2$ as the precursor with a mixed salt of $LiOH\text{-}LiNO_3$ as the lithium source under a flowing oxygen atmosphere at 700 °C[39]. The

LNO thus obtained possessed an excellent layered structure and hence a high capacity of 235.2 mAh g^{-1} upon charge/discharge at 0.1 C and a good capacity retention of ~80.2% after cycling at 1 C for 100 cycles.

The sol-gel method is characterized by the formation of a sol-gel network (as the precursor) from a solution containing the metal ions of the target cathode material, in which the sol-gel network is deduced through an appropriate means, such as hydrolysis reaction or chelating reaction[30,36,38]. In this method, a lithium source can be directly included into the precursor during the sol-gel formation, ensuring a uniform distribution of Li^+, bulk elements, and doping elements in the final cathode material[36,38]. For example, Kong *et al.* acquired a Cu-doped LNO gel precursor by dissolving $LiCH_3COOH$, $Ni(CH_3COOH)_2$, and $Cu(NO_3)_2$ in ethanol at 45 °C to obtain a Cu-LNO solution, followed by adding diacetone as the chelating agent and heating at 55 °C to initiate the chelating reaction[38]. Upon the solvent evaporation at 90 °C, the solution thus attained was converted into a green sol first and eventually the Cu-doped LNO gel as desired. Subsequently, calcinating this gel precursor under oxygen at 700 °C resulted in a coralline-like cathode material of $LiNi_{0.998}Cu_{0.002}O_2$. Thanks to its uniform elemental distribution achieved by the sol-gel process of the precursor, the as-synthesized $LiNi_{0.998}Cu_{0.002}O_2$ possessed a capacity of up to 218 mAh g^{-1} during the charge/discharge at 0.1 C in 2.5-4.5 V and showed excellent cycling stability with a capacity retention of 85% upon cycling at 0.5 C for 100 cycles.

In a hydrothermal process, the reaction of the precursor synthesis is carried out at a high temperature and under a high pressure self-generated in a closed system. By doing this, Essehli *et al.* firstly prepared a α-$3Ni(OH)_2{\cdot}2H_2O$ green powder in an autoclave containing a $Ni(NO_3)_2$ ethanol solution at 180 °C, followed by dispersing the α-$3Ni(OH)_2{\cdot}2H_2O$ thus prepared into an ethanol solution incorporating LiOH, $Al(NO_3)_3$, and $Mn(NO_3)_3$ to synthesize a precursor of $Ni_{0.9}Mn_{0.05}Al_{0.05}(OH)_2$@LiOH[40]. The proposed $LiNi_{0.9}Mn_{0.05}Al_{0.05}O_2$ cathode material was obtained by drying this precursor at 500 °C first and then calcinating at 750 °C and under oxygen. This cathode material was highly crystalline and had a large size for its spherical secondary particles (> 12 μm), which can deliver a capacity of up to 200 mAh g^{-1} during the charge/discharge at 0.3 C in 3.0-4.4 V and retain this capacity at 96% even after cycling for 100 cycles.

Using the co-precipitation method to synthesize a precursor is based on the co-precipitation of the bulk and doping elements of a target cathode material, in which an aqueous metal ion solution (with a designed stoichiometric ratio between the bulk and doping elements), a chelating agent (such as ammonium hydroxide), and a precipitant (such as NaOH or KOH) are simultaneously pumped into a continuously stirred reactor to precipitate all metal ions together into a mixed hydroxide as the precursor. In this procedure, while the coordination between the chelating agent and the metal ions is essential for ensuring the homogeneous elemental distribution, regulating the pH of the entire reaction system is critical for adjusting/optimizing the size and morphology of the primary/secondary particles of the precursor. Typically, a reaction time of over 20 hours is needed to achieve a high tap density and large secondary particles for the precursor. Using this approach, for instance, Cui *et al.* produced a spherical and large-sized $Ni_{0.94}Al_{0.05}Mg_{0.01}(OH)_2$ precursor (over 10 μm) from an aqueous solution containing $NiSO_4$, $Al(NO_3)_3$, and $MgSO_4$ using an ammonia-containing KOH solution to control the pH (11.0-11.5) and with a reaction time of 45-50 h[41]. The $LiNi_{0.94}Al_{0.05}Mg_{0.01}$ cathode material was obtained by calcinating the as-synthesized precursor with LiOH as the lithium source at 690 °C and under oxygen for 15 h. This cathode material consisted of element-uniformly-distributed, spherical, and large-sized secondary particles, presenting a high capacity of 210 mAh g^{-1} upon the charge/discharge at C/3 in 2.8-4.4 V along with a capacity retention up to 89% after cycling for 100 cycles.

As seen above, a range of methods have been developed for synthesizing CFNR cathode materials and are advantageous and disadvantageous on different aspects. In particular, the electrolytic method can produce cathode materials with a high purity and well-layered structure but requires extra efforts to deal with its accompanying hydrogen byproducts and electrolyte wastes; The sol-gel method ensures a uniform elemental distribution for the cathode materials but is relatively time-consuming (for solvent evaporation) and difficult to scale up; The hydrothermal strategy can obtain highly crystalline and large-particle-sized cathode materials but encounters with poor scalability and safety concerns (due to its high temperature-/high pressure-related reactions); The co-precipitation technique has the advantages of homogeneous distribution of elements, spherical shape and large size of dense particles, low cost, ease for continuous operation, and excellent scalability for production but needs to manage its liquid wastes. Overall, although different approaches should be selected to meet the varied property requirements for a specific cathode material, co-precipitation has been widely employed for the large-scale production of commercial layered oxide cathode materials including CFNR.

DEGRADATION OF CFNR CATHODE MATERIALS

Despite the significant advancements in the research of CFNR cathode materials, obstacles are still hindering the commercialization of these materials because of their degradations, mainly including crystal structure instability, phase transition, surface side reactions, and microcracking[4,20,42]. To obtain stable structural, mechanical, thermal, and electrochemical properties for CFNR cathode materials, it is of great importance to understand the mechanisms behind their degradations, which are comprehensively discussed as follows.

Crystal structure instability

A stable crystal structure is essential for Ni-rich layered oxide cathode materials including CFNR. Ideally, these materials should possess a well-defined crystal structure, where all elements in the lattice only play their unique roles without affecting each other. However, this is challenged by the issues mainly including Li/Ni mixing and oxygen loss of these materials, leading to their crystal structure instability.

Li/Ni mixing inherently exists in and has been attributed to similar ionic radii, superexchange interaction, magnetic frustration, and kinetic advantage of Ni-rich layered oxides[3,20,42].

Specifically, same as their prototype of LNO, Ni-rich layered oxides have an α-$NaFeO_2$-type hexagonal layered crystal structure ($R\bar{3}m$ space group), where the Li ions and TM ions are coordinated by oxygen to construct an alternately-arranged layered structure with Li and TM layers [Figure 3A][2]. The different sizes of Li^+ (0.76 Å) in the Li layers and Ni^{3+} (0.56 Å) in the TM layers are favorable for stabilizing the structures of these materials. However, the low valance state of Ni, i.e., Ni^{2+}, is always found in these materials, which has been largely attributed to the inadequate synthesis conditions during the precursor calcination of these materials (e.g., inappropriate temperature and deficient oxygen atmosphere)[13,43,44]. Also, the Ni^{3+}/Ni^{4+} generated on the surfaces of these materials during their charge/discharge can react with the electrolyte to produce Ni^{2+}[45,46]. As a result, due to their similar sizes in radii, Li^+ (0.76 Å) can enter into the TM slab and Ni^{2+} (0.69Å) into the Li slab, resulting in the so-called Li/Ni mixing[47,48].

Superexchange interaction refers to the enhanced exchange between two TM cations, one from the TM layer and the other from the Li layer, through a bridged anion (i.e., O^{2-}) of a layered oxide[26,49]. Through its unpaired spin electrons, the p orbitals of this intervening oxygen can bind with the d orbitals of the TM cations to form σ bonds. Using a Ni-rich layered oxide as the example [Figure 3B][26], the antisite Ni^{2+} in the Li layer tends to form a 180°-exchange interaction stronger with the Ni^{2+} than those with other metal ions in

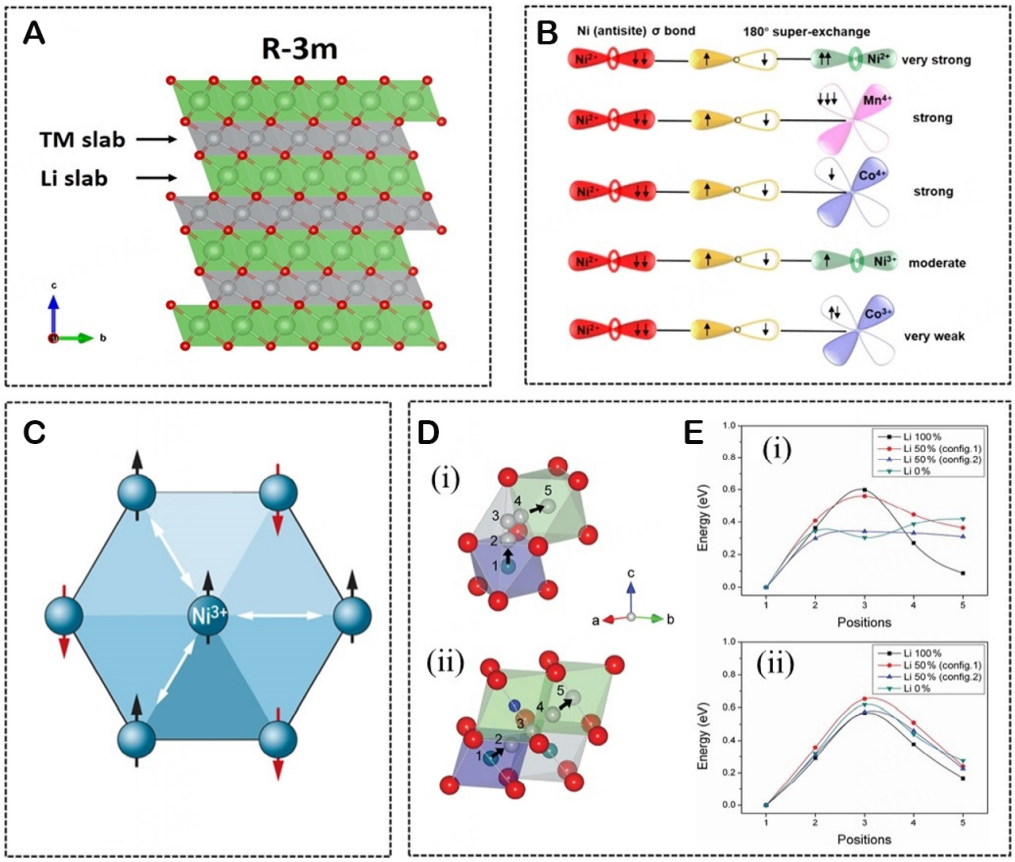

Figure 3. (A) Model of the layered structure with R$\bar{3}$m space group. This figure is quoted with permission from Yu *et al.*[2]. (B) Schematic for 180° superexchange interaction. This figure is quoted with permission from Zheng *et al.*[26]. (C) Schematic diagram of magnetic frustration effect. This figure is quoted with permission from Li *et al.*[25]. (D) Migration routes of Ni ions to Li sites in the layered structure for the Oh → Td → Oh route (i) and the Oh → V_O site → Oh route (ii), (E) Energy barriers calculated for migration of a Ni ion for the Oh → Td → Oh route (i) and the Oh → V_O site → Oh route (ii), the x-axis denotes the positions of Ni ions on the migration paths in (D). This figure is quoted with permission from Kim *et al.*[52].

the TM layer. Consequently, the preference of this interaction (due to its low energy) can enhance the Li/Ni mixing, which, in turn, makes the Ni-involved exchange interaction "super", resulting in the so-called superexchange interaction.

Magnetic frustration originates from the strong magnetic interaction due to the conflicting electron spins of TM ions in the hexagonal lattice of a TM layer. Using three triangularly placed Ni^{3+} (having their d shells half-filled) as the example [Figure 3C][25], the Ni^{3+} in the center of the hexagonal lattice has a spin state parallel (in the same direction) to those of its three surrounding Ni^{3+} at the apexes of the lattice. This arrangement of conflicting electron spins is a higher-energy and hence unstable state, leading to the so-called magnetic frustration that strengthens the Li/Ni mixing[50,51].

Kinetic advantage represents a situation in which the migration of Ni^{2+} from the TM layer to the Li layer has a low barrier in energy. Particularly, with $LiNi_{1-x}Co_xO_2$ as the example[52], the migration of Ni^{2+} from the TM layer to the Li layer is favorable to follow a route of O_h (octahedral Ni site)-T_d (tetrahedral site)-O_h (octahedral Li site) [Figure 3D(i)] owing to its low energy barrier of between 0.303 and 0.598 eV for the Li 0% (fully delithiated) and Li 100% (fully lithiated) states, respectively [Figure 3E(i)]. Even upon the oxygen loss of $LiNi_{1-x}Co_xO_2$, Ni^{2+} can also find a favorable path of Oh (Ni site)-Vo (oxygen vacancy)-Oh (Li site) for

migration [Figure 3D(ii)] because of its low energy barrier of between 0.567 and 0.617 eV for the Li 100% (fully lithiated) and Li 0% (fully delithiated) states, respectively [Figure 3E(ii)][52]. In this regard, compared to the migration of Co (e.g., with a high energy barrier in the route of O_h-T_d-O_h of 1.6 eV for $Li_{0.5}CoO_2$[53]), that of Ni^{2+} has a remarkably lower energy barrier and thus is considered kinetically advantageous for Li/Ni mixing[52].

Due to the strengthened Li/Ni mixing by the factors above, the crystal structures become unstable (with a decreased c parameter)[54], the Li^+ diffusion pathways are blocked (by the antisite Ni^{2+} in the Li slab)[1], the surface metals are lost (due to the migration of antisite Ni^{2+} to the particle surface)[26], and the layered structure is damaged (to disordered spinel and eventually rock salt)[55,56] for Ni-rich layered oxides.

Apart from Li/Ni mixing, oxygen loss is another important cause influencing the crystal structure instability of Ni-rich layered oxides[55]. Using the prototype of these materials (i.e., LNO) as the example, upon delithiation, its oxygen arrangement is transformed from the original face-centered cubic (O3, ABCABC) structure to the final hexagonal close-packed structure (O1, ABAB) [Figure 4A][55,57]. This transformation is accompanied by oxygen loss, which can be quantitatively interpreted by the formation energy of oxygen vacancy with thermodynamic calculations[58]. As can be seen in Figure 4B, the formation energy of oxygen vacancy of LNO decreases rapidly from 1.8 eV for the fully lithiated state to 0.35 eV for the 75% delithiated state, providing a strong driving force for oxygen loss.

Furthermore, oxygen loss promotes Li/Ni mixing, as depicted in Figure 4C, in which the oxygen loss-deduced vacancies (denoted as Vo) can reduce the energy barrier for the migration of their adjacent Ni ion from the Ni layer to the Li layer. Following the path of Oh-Td-Oh [Figure 4C], the migration energy barriers for a half-delithiated LNO with and without oxygen vacancies are calculated and plotted in Figure 4D[58], showing the strong effect of oxygen vacancies in reducing the energy barrier for Ni migration and thus enhancing the Li/Ni mixing.

As a result, along with the promoted Li/Ni mixing, oxygen loss destroys the crystal structures and produces unwanted gases, jointly leading to inferior electrochemical performance, poor thermal stability, and even safety hazards for Ni-rich layered oxides[52,55-60].

Phase transition

Along with their delithiation upon charge, Ni-rich layered oxide cathode materials, including CFNR, undergo a phase-transition sequence of Hexagonal 1 (H1) - Monoclinic (M) - Hexagonal 2 (H2) - Hexagonal 3 (H3) - Hexagonal 4 (H4) [Figure 5A][4,61]. The oxygen arrangement of the H1, M, H2, and H3 phases is in an O3 type but that of the H4 phase is in an O1 type. The presence of these phases during the charge/discharge of LNO, as an example, has been verified by the in-situ synchrotron diffraction, as shown in Figure 5B. Although a complete reversibility is desired for the transition between these phases, the real situation is complicated. Specifically, at a high delithiation state ($x > 0.95$), the layered slip of the H3 phase results in the formation of the H4 phase (NiO_2, CdI_2-type structure), unfortunately creating lattice mismatch and volume changes that can impede Li^+ transport and degrade the cathode materials[23]. In practice, therefore, the cutoff voltage during charge (i.e., the depth of delithiation) is usually limited to avoid the appearance of the H4 phase for these materials[7,8,11].

During lithiation/delithiation, largely owing to their smaller change in lattice structure (using the c-axis parameter change as the example as shown in Figure 5A), the transition among the H1 → M → H2 phases is more reversible than that between the H2 → H3 phases[11,62]. Indeed, upon the increased depth of

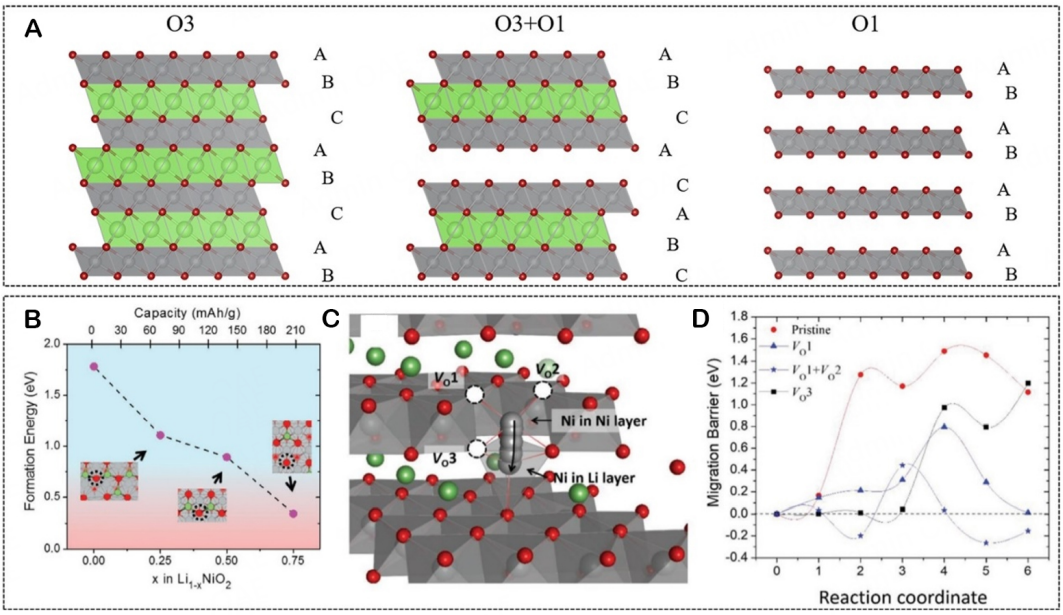

Figure 4. (A) Atomic models of O3 phase (space group $R\bar{3}m$), O3 phase with partially transited O1 phase, and pure O1 phase. Li, Ni, and O are denoted by green, gray, and red symbols, respectively. This figure is quoted with permission from Wang *et al.*[55]. (B) Oxygen vacancy formation energy during delithiation of $LiNiO_2$, (C) Configuration for Ni migration in $Li_{0.5}NiO_2$, Vo1, Vo2, and Vo3 represents oxygen vacancies neighboring with diffusive Ni ion, (D) The migration barriers for Ni ions to diffuse from transition metal layer to Li layer, under different situations (Pristine: no neighboring oxygen vacancy; Vo1: with neighboring vacancy Vo1; Vo1 + Vo2: with neighboring vacancies Vo1 and Vo2; Vo3: with neighboring vacancy Vo3). This figure is quoted with permission from Kong *et al.*[58].

delithiation, the H2 → H3 transition can cause a large anisotropic contraction (as schematically presented by the dramatic decrease in the c-axis parameter in Figure 5A) and hence the collapse of the layered structure. This structural strain, in turn, induces inter-/intra-granular cracking, loss of interparticle contact, and loss of active materials through defect and rock-salt formation, thereby leading to inferior and irreversible electrochemical performance for the cathode materials[1,63]. Therefore, owing to its great impact on the structure stability and electrochemical performance, the H2 → H3 phase transition for Ni-rich layered oxide cathode materials, including CFNR, has been extensively studied and should be paid more attention in the future research[9,11].

Surface side reactions

An ideal surface able to ensure the stable mechanical, thermal, and electrochemical properties is required for Ni-rich layered oxide cathode materials including CFNR. In practice, however, this remains challenging because of the possible surface side reactions of these materials attributable to their high reactivities with the electrolyte and the environment.

On the one hand, the high reactivity of these materials refers to $Ni^{3+/4+}$ generated upon their delithiation to a highly-charged state, which can react with the electrolyte to produce the undesirable species such as Ni^{2+}, O_2, and CO_2[15,42]. While the generated Ni^{2+} can enhance the Li/Ni mixing to deteriorate the crystal structure, the generated O_2 means oxygen loss and induced crystal structure instability for these materials; both have been discussed under Section "Crystal structure instability". Moreover, all gases produced imply the gassing inside the battery that may cause serious safety hazards[46]. The surface of the cathode materials is prone to erosion/dissolution by HF derived from the $LiPF_6$ decomposition and hydrolysis of the electrolyte, leading to the loss of active TM and, hence, the capacity degradation for these materials[64]. Also, the dissolved TM can be reduced into metals and participate in forming a solid electrolyte interface (SEI) on the anode. These

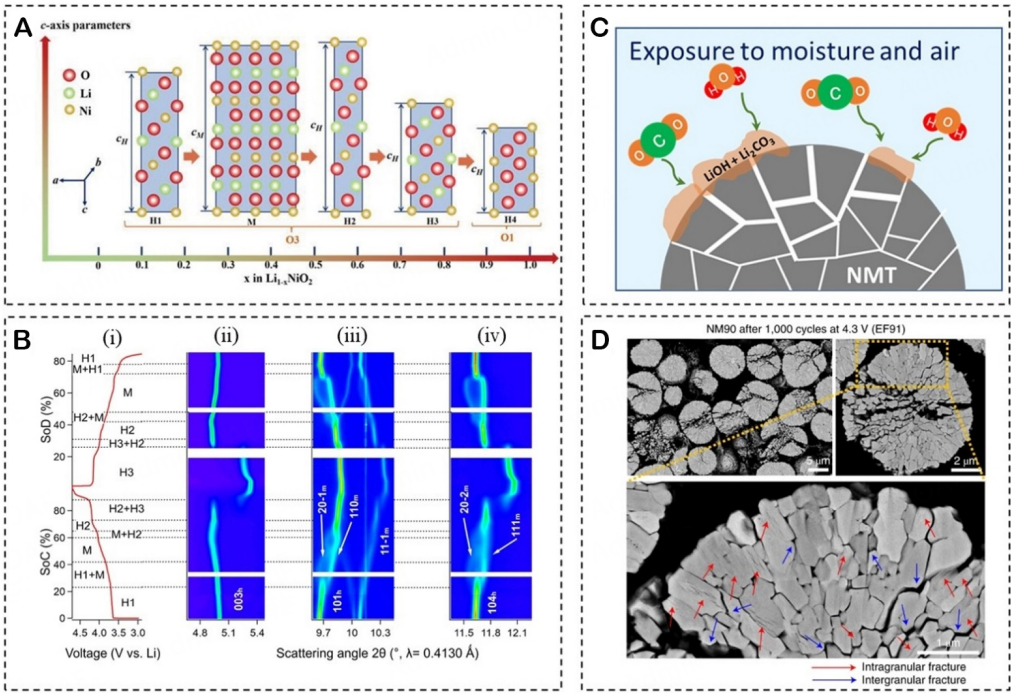

Figure 5. (A) Schematic diagram of the structural evolution (H1 → M → H2 → H3 → H4) during the charging of layered $LiNiO_2$ materials. This figure is quoted with permission from Li *et al.*[4]. (B) Contour maps of in situ synchrotron diffraction of LNO collected during the first cycle. Cell voltage as a function of state of charge or discharge of the first cycle, which is aligned with the diffraction patterns (i). XRD patterns of selected scattering angle regions: 4.68°-5.48° (ii), 9.59°-10.45° (iii), and 11.36°-12.26° (iv). Based on the refinement results, the phases in each region are labeled in (i). The peak splitting for phase M is also indicated in (iii) and (iv). This figure is quoted with permission from Li *et al.*[61]. (C) Illustration of the reactions of the surface residual lithium of a $LiNi_{0.96}Mg_{0.02}Ti_{0.02}O_2$ (NMT) cathode with H_2O and CO_2 in the air, forming LiOH and Li_2CO_3, respectively. This figure is quoted with permission from Kim *et al.*[15]. (D) Cross-sectional SEM images of a $LiNi_{0.9}Mn_{0.1}O_2$ (NM90) cathode after 1,000 cycles in full cells featuring EF91 electrolyte, cycled in the voltage range of 3.0-4.3 V. This figure is quoted with permission from Park *et al.*[9].

will hinder the Li^+ intercalation into the anode and disrupt the original cathode/anode capacity ratio, thereby raising the impedance and deteriorating the battery performance[64].

On the other hand, the high reactivity of these materials is expressed by their environmental instability. Specifically, the residual lithium on the surface of these materials, which is left during the material synthesis[46,65], can initiate some unwanted side reactions, such as those with H_2O and CO_2 in the air to form LiOH and Li_2CO_3, respectively [Figure 5C][15]. In the subsequent slurry process for electrode preparation, the LiOH and Li_2CO_3 thus formed can react with polyvinylidene fluoride (PVDF), the commonly used binder for cathodes, to form gels that will increase the difficulty and even disable the production of the electrodes[65,66]. Therefore, cathode materials without any side reactions with the electrolyte and the environment are highly desired.

Microcracking

Mechanical stability/integrity of Ni-rich layered oxide cathode materials including CFNR play an important role in ensuring their stable electrochemical performance. This is, however, affected by a mechanical degradation mechanism (called microcracking) that occurs during the charge/discharge of these materials[67,68]. Typically, the secondary particles of layered oxides comprise multiple primary particles in the size of sub-micrometers (even nanometers)[7,67]. Upon charge/discharge, the Li^+ intercalation/deintercalation into/out of these materials may cause expansion and contraction in volume for their primary particles,

resulting in intragranular fracturing within and intergranular fracturing between the primary particles (i.e., microcracking) as marked in Figure 5D by red and blue arrows, respectively[9]. The continuous expansion and contraction of the primary particles exacerbate the growth of the intergranular fractures (microcracks) to form isolated particles. Without contact with the electrolyte, these isolated particles cannot undergo Li^+ intercalation/deintercalation and hence become electrochemically inactive. As a result, microcracking will deteriorate the mechanical stability/integrity and degrade the electrochemical performance of the cathode materials[67,68].

Moreover, upon charge/discharge cycling, the proliferation of microcracks allows the electrolyte to infiltrate/penetrate into the newly formed surfaces, making the surface side reactions, as discussed under Section "Surface side reactions", occur inside the particles of the cathode materials, further degrading their electrochemical performance and even causing safety issues for batteries[55]. Therefore, mechanically stable/complete cathode materials able to suppress such kind of microcracking are highly desired.

The degradation mechanisms of Ni-rich layered oxide cathode materials including CFNR discussed above can occur individually and interact with each other. The appearance of one mechanism may trigger others to occur, jointly deteriorating the structural, mechanical, thermal, and electrochemical properties of these materials and even deducing safety hazards for their batteries. Therefore, when researching a new strategy for improving the properties for CFNR cathode materials, these degradation mechanisms should be thoroughly considered/addressed.

MODIFICATION FOR CFNR CATHODE MATERIALS

In order to enhance the structural, mechanical, thermal, and electrochemical properties of CFNR cathode materials towards their practical applications, considerable efforts have been made in recent years to address the degradations of these materials, as discussed above[2,3,41,68-73]. Among them, the modification strategies of bulk-phase doping, surface coating, and single crystallization have been extensively studied, to be elucidated as follows.

Bulk-phase doping

Bulk-phase doping refers to incorporating small amounts (typically less than 5%) of additional elements as dopants into the host lattice of a cathode material without introducing impurity phases. With this strategy, substantial efforts have been made to dope non-Co elements into Ni-rich layered oxides to fabricate CFNR cathode materials[2,3,18,19,44,74-81]. This has been demonstrated to be effective in stabilizing the crystal structure and suppressing the phase transition to enhance the properties for CFNR cathode materials[7,9]. In this regard, as schematically presented in Figure 6A, bulk-phase doping has been realized for CFNR cathode materials on a range of locations including Ni-site (TM layer), Li-site (Li layer), Ni/Li dual-sites, O-site, and interstitial sites[16,27,71,72,77,81-85].

Ni-site doping has been considerably studied for CFNR cathode materials owing to its effectiveness in strengthening the metal-oxygen binding thus suppressing the Li/Ni mixing, oxygen loss, and phase transition[16,19,36,77,84,86]. It can be carried out either during the synthesis of precursors or in the calcination of the pre-formed precursors. In the former, the dopant ions are introduced into the bulk metal salt solution to prepare precursors, followed by calcinating the precursors thus obtained with a lithium source to produce the cathode materials[8,41,87]. This allows the uniform distribution of dopants in the cathode materials. The latter physically mixes the dopants with the pre-formed precursors and a lithium source, followed by calcination to produce the cathode materials[9,10,16,30]. A large variety of metal ions having ionic radii similar

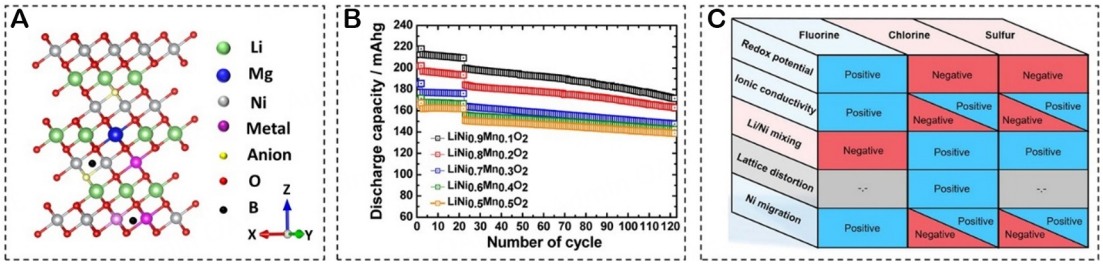

Figure 6. (A) Schematic diagram of possible doping sites on a CFNR cathode material. (B) Capacity retention of the Ni-rich $Li(Ni_{1-x}Mn_x)O_2$ ($0.1 \leq x \leq 0.5$) electrodes in a voltage window of 2.7-4.3 V at 30 °C for 120 cycles. 1-20 cycles: 0.2 C; and 21-120 cycles: 0.5 C. This figure is quoted with permission from Sun *et al.*[7]. (C). Summary of anion doping effects on the battery performance of LNO. This figure is quoted with permission from Kong *et al.*[84].

to that of Ni^{3+} (0.56 Å) have been employed for Ni-site doping, which, depending on their valence states, can be classified into low- and moderate-valence dopants, respectively.

Fe^{3+} and Al^{3+} are frequently used low-valence dopants for Ni-site doping for CFNR cathode materials[18,38,77,88,89]. For example, Xi *et al.* used Fe^{3+} as the dopant to replace Co^{3+} of NCM811 to prepare a new CFNR cathode material of $LiNi_{0.8}Fe_{0.1}Mn_{0.1}O_2$[89]. With a traditional co-precipitation method, Fe was first incorporated into the hydroxide precursor with Ni and Mn, followed by calcinating the resultant precursor with LiOH to produce the target $LiNi_{0.8}Fe_{0.1}Mn_{0.1}O_2$. Even without Co, this material realized a low energy barrier of Li^+ diffusion (0.969 eV), similar to that of NCM811 (0.979 eV), thus exhibiting a high capacity of 202.6 mA h g^{-1} at 0.1 C in 3.0-4.5 V and a capacity retention up to 81.1% after 10 C cycling for 150 cycles in 3.0-4.3 V.

Moderate-valence dopants, such as Zr^{4+}, Ti^{4+}, and Mn^{4+}, are also employed for Ni-site doping for CFNR cathode materials, which is largely encouraged by their capability to form strong TM-O bonds[7,18,78,90,91]. Among them, Mn^{4+} has been paid more attention[7,31,78]. For instance, Sun *et al.* studied the effect of the Mn^{4+} dopant using the conventional co-precipitation process to prepare a range of $Ni_{1-x}Mn_x(OH)_2$ ($0.1 \leq x \leq 0.5$) precursors, followed by calcinating these precursors with $LiNO_3$/LiOH to obtain the $LiNi_{1-x}Mn_xO_2$ ($0.1 \leq x \leq 0.5$) cathode materials[7]. These materials comprised dense and spherical secondary particles with high crystallinity and thus low cation mixing. Therefore, having the lowest cation mixing (2.9%), the optimized composition, i.e., $LiNi_{0.9}Mn_{0.1}O_2$, delivered a capacity of up to 200 mAh g^{-1} at 0.5 C (2.7-4.3 V, 30 °C) and retained this capacity at ~86% after cycling for 100 cycles [Figure 6B]. Nevertheless, it should be noted that doping of the moderate-valence elements (along with their induced charge imbalance) may result in the formation of Ni^{2+} and hence the promoted Li/Ni mixing[31,90]. This indicates a need for the careful content optimization of moderate-valence elements when doping them into CFNR cathode materials.

Similarly, with its ionic radius close to that of Li^+ (0.76 Å)[39], Mg^{2+} (0.72 Å) was extensively studied for doping the Li-site of CFNR cathode materials[85,92-95]. Indeed, Mg^{2+} has been demonstrated to be effective as a pillar ion in mitigating the internal stress of the crystal lattice during the anisotropic lattice contraction at a high charging state, thereby enhancing the structural stability and electrochemical performance for CFNR cathode materials[92,96]. For instance, Laine *et al.* used co-precipitation to incorporate varied amounts of Mg^{2+} into $Ni(OH)_2$, the hydroxide precursor of LNO, followed by calcinating the precursors thus prepared with LiOH to produce Mg-doped LNO cathode materials[95]. Although having a lowered initial capacity at 0.1 C in 3.0-4.3 V, these Mg-modified materials displayed a significantly enhanced cycling stability, for example, with the boosted capacity (198.3 *vs.* 193.6 mAh g^{-1}) and capacity retention (98.9% *vs.* 87.6%) for a 2 mol% Mg-doped LNO cathode over its pristine counterpart in the subsequent cycling for 62 cycles.

Logically, combing their benefits as elucidated above, Ni-site doping and Li-site doping have been conducted simultaneously, resulting in a range of Ni/Li dual-site doping combinations, such as Al/Mg[41,97], Ti/Mg[55,81,96], and Mn/Mg[72], to further improve the properties for CFNR cathode materials. For example, Mu *et al.* prepared a Ni/Mg/Mn-incorporating hydroxide precursor via co-precipitation first and then calcinated the as-prepared precursor with LiOH to synthesize a Mg/Mn-LNO cathode material[72]. Owing to the occupations of Mg^{2+} on the Li site and Mn^{4+} on the Ni site, respectively, for co-doping, the Mg/Mn-LNO cathode delivered a smooth voltage profile, enhanced structural stability, elevated self-discharge resistance, and inhibited nickel dissolution. These enabled the Mg/Mn-LNO cathode with improved cycling stability, presenting high capacity retentions of 80% after 350 cycles at C/3 and 67% after 500 cycles at 2 C in 2.5-4.4 V.

Apart from cation doping on the metal sites, as discussed above, anion doping on the O-site has also attracted considerable attention for CFNR cathode materials, with the frequently studied anions being F, Cl, and S[84,98]. Although anion doping can be expected to enhance the properties for cathode materials, the selection of anions should be carefully considered because of their possible conflicting effects. In this regard, Kong *et al.* used density functional theory (DFT) to systematically investigate the effects of F, Cl, and S on the properties (including redox potential, ionic conductivity, Li/Ni exchange, lattice distortion, and Ni migration upon delithiation) of LNO as a model cathode material[84]. As schematically summarized in Figure 6C, while F can improve almost all the properties considered, it, unfortunately, facilitates the Li/Ni mixing due to its reduced energy in forming the Li/Ni defects. With their increased Li/Ni defect formation energies, in contrast, Cl and S can suppress the Li/Ni mixing and lattice distortion (especially Cl). However, concerning F, Cl- and S-dopings result in lower redox potentials for their doped LNO, which is attributed to their relatively weaker bonding strength with Li. Moreover, Cl and S have contradictory effects on the structural stability and rate capability for LNO; that is, a high doping concentration can benefit the former whereas a low one is preferred for the latter. To address the conflicting effects from anion doping, a codoping strategy by coming anion doping with cation doping has been suggested for Ni-rich layered oxide cathode materials including CFNR[84].

Unlike the doping on a specific site, such as the Ni-site, Li-site, or O-site, as discussed so far, interstitial doping refers to that within the space between varied atoms of a cathode material [Figure 6A][71,99], which is usually achieved by boron (B)[16,71]. B-doping has been considered effective in microstructurally engineering the primary particles of a cathode material. Specifically, it can dissolve (insert) into the host structure, leading to a surface-confined distribution to inhibit the growth and hence increase the aspect ratio (length/diameter) for the primary particles of the cathode material. This significantly enhances the microstructural and hence cycling stabilities for CFNR cathode materials. For example, Kim *et al.* doped B into LNO by firstly synthesizing a $Ni(OH)_2$ precursor via co-precipitation and then calcinating the pre-synthesized precursor with B_2O_3 and LiOH to fabricate a B-doped LNO (i.e., B-LNO) cathode[71]. In a full-cell configuration (with a graphite anode), this B-LNO cathode showed an initial capacity of 200 mAh g^{-1} and retained this capacity up to 81% even after cycling for 300 cycles (0.5 C, 2.7-4.2 V), significantly outperforming its pristine counterpart (having a similar initial capacity but a lower capacity retention of about 71%).

Surface coating

Surface coating is a strategy that applies a protective layer on the surface of CFNR cathode materials to protect them from the direct contact with the electrolyte and the environment to suppress the side reactions for enhancing their properties[15,69,73,100]. Generally, this method can be carried out on either the secondary or primary particle surface of a target CFNR cathode material.

Secondary particle coating refers to applying a modifying material directly onto the secondary particle surface of a CFNR cathode material. This has been practiced for years with various materials, such as metals, metal oxides, polymers, and carbon/polymer composites, as illustrated below.

For coating metals on CFNR cathode materials, Chu *et al.* developed a method by combining solid-phase mixing with low-temperature sintering to coat a 35 nm-thick selenium (Se) metallic coating on LNO to fabricate a Se-LNO cathode [Figure 7A][73]. Owing to its stabilized interface and enhanced kinetic behavior and the suppressed phase transition, particle pulverization, and HF corrosion enabled by the Se coating, this Se-LNO cathode showed an improved rate capability (capacity at 5 C: 149.6 *vs.* 135.7 mAh/g) and cycling stability (capacity retention after 300 cycles at 1 C: 82.09% *vs.* 31.31%) over its pristine counterpart.

Inspired by the previous research about the capability of a metal oxide coating of Al_2O_3 to enhance the properties of layered oxides[101-105], Kang *et al.* used first-principles calculations to investigate how Al_2O_3 can improve the thermal stability of CFNR cathode materials[100]. With the archetype cathode of LNO, their study indicated that the Al_2O_3 deposits undergo a phase transition from the corundum-type crystalline (c-Al_2O_3) to amorphous (a-Al_2O_3) structures as the number of coating layers reaches three. The resultant a-Al_2O_3, in turn, can significantly suppress the oxygen evolution of LNO at 400 K, which is apparently different from the situation of the pristine LNO that immediately releases oxygen upon its exposure within a very short period time of 1 ps at the same temperature. The authors verified the underlying mechanism of this significance to be the strong contacting force at the interface between LNO(012) and Al_2O_3 deposits that originates from the highly ionic chemical bonding of Al and O at the interface.

To pursue the polymer coating strategy for CFNR cathode materials, Kim *et al.* mechanically mixed $LiNi_{0.96}Mg_{0.02}Ti_{0.02}O_2$ (NMT) powder in a polyimide/polyvinylpyrrolidone (PI/PVP, denoted as PP)-containing N-methyl-2-pyrrolidone (NMP) solution, followed by a stepwise imidization process to remove the remained NMP solvent to fabricate a PP-coated NMT (PP@NMT) cathode[15]. Due to the high thermal stability of PI and the high Lewis basicity (to scavenge HF of the electrolyte) of PVP, the resultant dual-protection PP layer enabled the PP@NMT cathode with the superior resistances to the surface contamination in moist air and the interfacial side reactions upon cycling. As a result, the PP@NMT cathode preserved a relatively clean surface with the bare generation of lithium residues, structural degradation, and gas evolution even after exposure to air with ~30% humidity for two weeks compared to the bare NMT, and exhibited a high capacity retention of 86.7% (*vs.* 63.2% for the bare NMT) after 500 cycles at C/3 using a localized high-concentration electrolyte [Figure 7B].

To study carbon/polymer composite coatings for CFNR cathode materials, Luu *et al.* prepared a graphene-ethyl cellulose (GrEC)-coated LNO cathode by firstly dispersing LNO powder in a GrEC-containing NMP solution and then casting the resultant dispersion directly onto an Al foil to fabricate the electrode[69]. The hydrophobic property of the GrEC composite was demonstrated to be effective in protecting the LNO surface from the contact with atmospheric moisture, thereby minimizing the lithium impurity generation and hence enhancing the electrochemical performance for the LNO electrode thus modified[69]. Even upon exposure to humidified CO_2 for 24 h, the GrEC-coated LNO electrode delivered a capacity of 230 mAh g^{-1} (0.1 C, 2.8-4.6 V), slightly lower than that of the electrode without CO_2 exposure (240 mAh g^{-1}). When compared to the significant capacity degradation of the pristine LNO electrode from 240 to 180 mAh g^{-1} upon the CO_2 exposure, this clearly highlights the effectiveness of the carbon/polymer composite coatings for CFNR cathode materials.

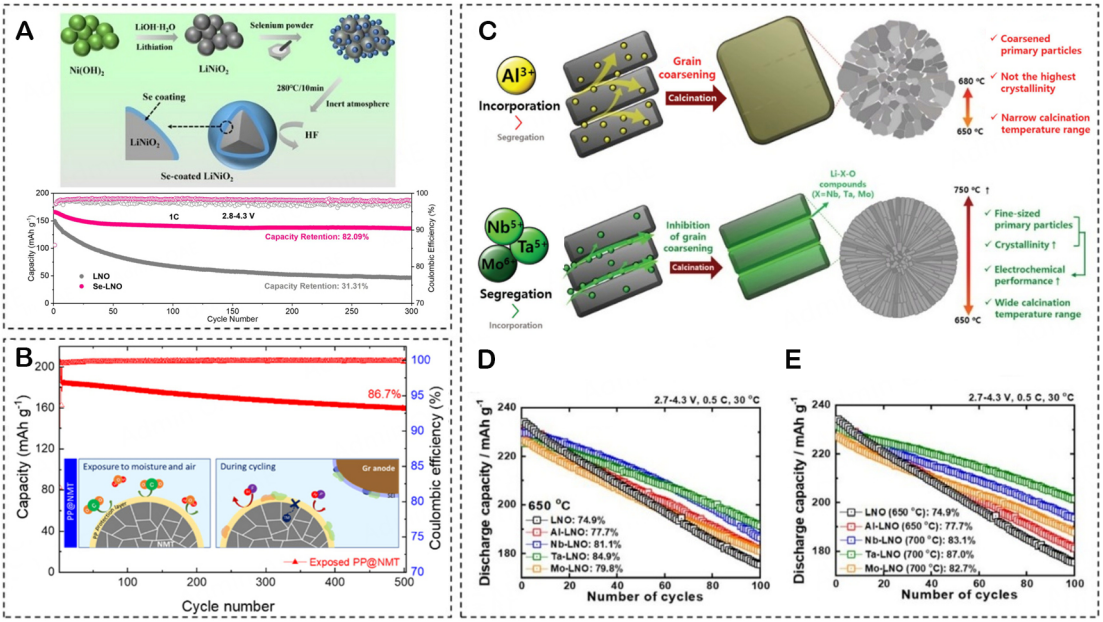

Figure 7. (A) Schematic diagram of the synthesis process for Se-LNO. Long-term testing of LNO and Se-LNO at 1 C and cutoff voltages of 2.8-4.3 V over 300 cycles. This figure is quoted with permission from Chu *et al.*[73]. (B) Schematic illustration of the advantages and cycling performance of the dual-protection PP-coating layer. This figure is quoted with permission from Kim *et al.*[15]. (C) Differences in mechanism and effects of low-valence (Al) and high-valence (Nb, Ta, and Mo) dopants, including the incorporation into bulk and the grain boundary coating, (D and E) Cycling performance (0.5 C, 2.7-4.3V) of half-cells featuring LNO, Al-LNO, Nb-LNO, Ta-LNO, and Mo-LNO cathodes calcined at 650 °C (D) and their respective optimized calcination temperatures (E). This figure is quoted with permission from Park *et al.*[10].

With respect to secondary particle coating, primary particle coating is an emerging method, in which the coating materials are directly cladded on the surface of the primary particles of a CFNR cathode material. Direct coating at the primary particle level has been demonstrated to possess some unique advantages as elucidated below.

One approach to realizing primary particle coating is conducted by crushing the secondary particles of a cathode material into primary particles first, followed by coating the primary particles thus formed with a modifying material. For instance, Brow *et al.* first milled the secondary particles of $LiNi_{0.9}Mn_{0.05}Al_{0.05}O_2$ into primary particles and then used H_3PO_4 to react with the surface residual lithium of the resultant primary particles to form a Li_3PO_4 layer on the primary particles[106]. Benefiting from the enhanced air stability and suppressed electrolyte-side reactions by the Li_3PO_4 layer, the $LiNi_{0.9}Mn_{0.05}Al_{0.05}O_2$ thus modified showed a remarkably enhanced cycling stability (especially at a high voltage) with a capacity of 180 mAh g^{-1} (*vs.* 100 mAh g^{-1}) after 100 cycles at C/3 in 2.8-4.6 V over its pristine counterpart. However, as can be seen, this method needs to crush secondary particles before the coating on primary particles, which inevitably damages the morphology of the secondary particles and, likely, the structure of the primary particles. It also requires extra time for processing and thus raises the practical application cost.

Without crushing the secondary particles, another approach for primary particle coating is achieved by forming the coating in situ during the calcination process of a cathode material. Specifically, this can be done by mixing a $Ni(OH)_2$ precursor with LiOH and the oxide (or hydroxide) of a high-valence element (such as Nb^{5+}, Ta^{5+}, W^{6+}, or Mo^{6+}), followed by calcination under oxygen at a high temperature[9,10,14,17,70,74,76,80,107-109]. As schematically illustrated in Figure 7C, unlike the doping of low-valence elements into the bulk structure, these high-valence elements usually accumulate (due to their insolubility

into the crystal structure[10]) along the interparticle boundaries and form Li-X-O compounds (due to their high electronic hybridization with oxygen[108]) there to accomplish the coating on primary particles. Since the temperature at which the content of Li-X-O compounds declines is higher for high-oxidation-state dopants, the segregation at the grain boundary can be reinforced, the size of primary particles can be refined, and the calcination temperature range can be widened for high-valence-element-doped CFNR cathode materials, thereby maintaining their highly aligned microstructure and high crystallinity over a wide calcination temperature range[10]. Furthermore, the grain size refinement achieved by high-valence-element doping dissipates the deleterious strain from abrupt lattice contraction through fracture toughening and the removal of local compositional inhomogeneities, and the enhanced cation ordering induced by the presence of high-valence elements stabilizes the delithiated structure through a pillar effect[9]. Together, these boost the cycling stability for high-valence-element-doped CFNR cathode materials. Using this strategy, Park *et al.* doped LNO with Nb^{5+}, Ta^{5+}, and Mo^{6+}, respectively, by calcinating their oxides with a $Ni(OH)_2$ precursor (pre-prepared via co-precipitation) and LiOH[10]. They clearly demonstrated the superior cycling stability of the resultant Nb-LNO, Ta-LNO, and Mo-LNO cathodes over the pristine and a low-valence-element-doped (i.e., Al-LNO) counterparts regardless of the calcination temperatures (either at a same temperature of 650 °C [Figure 7D] or their respective optimized calcination temperatures [Figure 7E]. Importantly, these works spotlight the excellence of primary particle coating (through high-valence-element doping) in facilitating the practical applications of CFNR cathode materials.

Single crystallization

Single crystallization is a strategy that synthesizes the CFNR cathode materials in a single crystal structure to stabilize the mechanical structure/integrity for improving the properties of these materials[110]. As discussed earlier under Section "Microcracking" and now schematically illustrated in Figure 8A, upon the microcracking during the charge/discharge of a conventional polycrystalline cathode material, its resultant intergranular fractures (microcracks) allow the electrolyte to infiltrate/penetrate into the newly formed surfaces of the material. This, in turn, promotes a series of issues including surface side reaction, surface pulverization, structure collapse, disordered phase transition, TM dissolution, and cathode/electrolyte interface (CEI) thickening, and eventually degrades the electrochemical performance and may cause safety concerns for this cathode material.

Although the strategies of bulk-phase doping[111,112] and surface coating[113-115] can alleviate the microcracking to some extent, single crystallization has been demonstrated to be the most effective in doing so[116,117]. Particularly, since single crystal structures can eliminate the uneven stresses deriving from the intergranular boundaries of polycrystalline structures, single crystallization has been extensively studied to suppress the microcracking-induced issues of polycrystalline materials [Figure 8A] and, more excitingly, to synthesize single crystal CFNR cathode materials in recent years[67,86,87,93,118-120].

Single crystal CFNR cathode materials can be synthesized using a solid-phase calcination process similar to polycrystalline materials. However, since the calcination temperature for a single crystal cathode material is always higher than that for its polycrystalline counterpart, which would result in lithium evaporation and serious Li/Ni mixing[68], a low-melting-point lithium salt (in addition to the lithium source used in the conventional solid-phase calcination process) is usually introduced to form a molten salt mixture to facilitate the single crystal growth through a dissolution-recrystallization mechanism[68,118,119]. For example, Dai *et al.* developed a LiOH-Li_2SO_4 molten salt method to synthesize a single crystal $LiNi_{0.9}Mn_{0.1}O_2$ (SC-NM91) cathode material[67]. Specifically, SC-NM91 was obtained by calcinating its $Ni_{0.9}Mn_{0.1}(OH)_2$ precursor (pre-prepared via co-precipitation) in a LiOH-Li_2SO_4 molten salt mixture. For comparison, the polycrystalline $LiNi_{0.9}Mn_{0.1}O_2$ (PC-NM91) was synthesized with the traditional solid-phase calcination process without Li_2SO_4. Upon the single crystal formation, the characteristic microstructure of the spherical

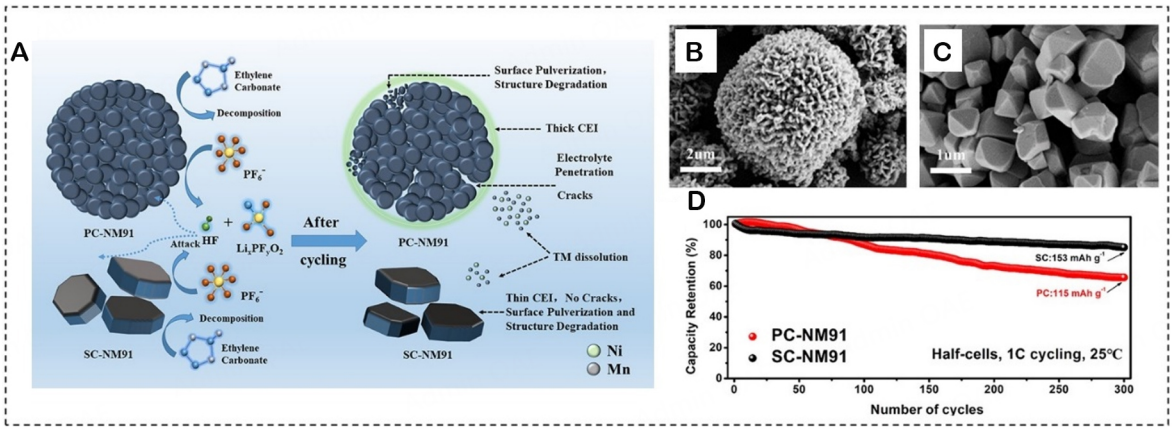

Figure 8. (A) Schematic illustration for the mechanism of single crystal structure mitigating the structure degradation and performance deterioration of $LiNi_{0.9}Mn_{0.1}O_2$ (NM91), (B and C) SEM images of PC-NM91 (B) and SC-NM91 (C), (D) Half-cell cycling tests of PC-NM91 and SC-NM91using Li as the anodes. This figure is quoted with permission from Dai *et al*.[67].

secondary particles of PC-NM91 [Figure 8B] vanished and a single granular morphology with complete/uniform structure and good dispersion appeared for SC-NM91 [Figure 8C]. As a result, owing to its strengthened structure able to overcome the microcracking-induced issues of polycrystalline cathode materials as illustrated in Figure 8A, SC-NM91 showed excellent cycling stability (capacity retention after 300 cycles at 1 C in 3.0-4.3 V: 87.72% *vs.* 65.53%), significantly outperforming its PC counterpart [Figure 8D]. More importantly, this emphasizes the benefit of single crystallization in enhancing the mechanical stability/integrity and hence electrochemical performance for CFNR cathode materials[67,86,87,93,118-120].

As seen above, various modification strategies have been considerably studied to improve the properties of CFNR cathode materials. While bulk-phase doping into various sites can stabilize the crystal structure and restrain the phase transition, surface coating on secondary and primary particles can suppress the side reactions, and single crystallization can strengthen the mechanical stability/integrity for these materials. Moreover, regarding the varied degradation mechanisms of CFNR cathode materials that may trigger each other to take place simultaneously, different modification strategies can/should be incorporated together to jointly overcome these problems to efficiently enhance the overall structural, mechanical, thermal, and electrochemical properties of these materials, towards their practical applications.

CONCLUSIONS AND OUTLOOKS

The rapidly increasing demands in lowering the cost and enhancing the energy density have continuously facilitated the research and development of new cathode materials for LIBs, to which CFNR cathode materials are considered good candidates largely owing to their low cost and high capacity. Among the diverse methods for synthesizing these materials, co-precipitation has been widely employed due to its distinct advantages over electrolytic, sol-gel, and hydrothermal approaches. However, in order for CFNR cathode materials to be practically useful for LIBs, their degradation issues, mainly including crystal structure instability, phase transition, surface side reactions, and microcracking, should be thoroughly considered and solved.

In this regard, extensive research has been conducted in the past years to address these shortcomings of CFNR cathode materials. Specifically, bulk-phase doping with non-Co elements has been performed on various sites including Ni-site, Li-site, Ni/Li dual-sites, O-site, and interstitial sites to stabilize the crystal

structure and restrain the phase transition for these materials. Surface coating on either the secondary or primary particles of these materials has been demonstrated to be effective in protecting them from the direct contact with the electrolyte and the environment to suppress their side reactions. Single crystallization can synthesize these materials in a single crystal structure to strengthen their mechanical stability/integrity to overcome the microcracking-deduced problems. Provided their effectiveness has already been demonstrated and drawbacks still exist, these modification strategies are worth further investigation to better improve the structural, mechanical, thermal, and electrochemical properties for CFNR cathode materials. Moreover, since the different degradation mechanisms of these materials may interact with each other to occur simultaneously, various combinations of these modification strategies should be considered accordingly, which can jointly enhance the overall properties and indeed represent a future research direction for CFNR cathode materials. Furthermore, owing to their merits that have been demonstrated in enhancing the properties of conventional layered oxides, core-shell[121-123] and gradient-concentration structures[18,124] are worth being studied for CFNR cathode materials with new structures. Finally, towards the practically useful applications of CFNR cathode materials at the industrial level, their future research should be rationally expended with binders[125-128] and electrolytes[15,45] because the former are an essential component for electrode fabrication and the latter for cell assembly, both influencing the electrochemical performance of CFNR cathode materials.

Given their remarkable advancements accomplished in the past and the considerable research under development, it is anticipated that high-performance CFNR cathode materials will emerge as the next-generation cathode materials to meet the ultimate goal for producing low-cost and high-energy LIBs.

DECLARATIONS

Authors' contributions

Writing - original draft: Wen L
Data analysis and interpretation: Wang X, Zeng X, Wang T, Li L, Hu Y, Yu Q
Writing - review & editing: Cheng F, Lu W
Funding acquisition, project administration, resources, supervision: Lu W

Availability of data and materials

Not applicable.

Financial support and sponsorship

This work was financially supported by Major Science and Technology Projects in Yunnan Province (grant number: 2016HE001-2016HE002).

Conflicts of interest

All authors declared that there are no conflicts of interest.

Ethical approval and consent to participate

Not applicable.

Consent for publication

Not applicable.

REFERENCES

1. Lee S, Manthiram A. Can cobalt be eliminated from lithium-ion batteries? *ACS Energy Lett* 2022;7:3058-63. DOI
2. Yu L, Liu T, Amine R, Wen J, Lu J, Amine K. High nickel and no cobalt - the pursuit of next-generation layered oxide cathodes. *ACS Appl Mater Interfaces* 2022;14:23056-65. DOI
3. Kim Y, Seong WM, Manthiram A. Cobalt-free, high-nickel layered oxide cathodes for lithium-ion batteries: progress, challenges, and perspectives. *Energy Stor Mater* 2021;34:250-9. DOI
4. Li H, Wang L, Song Y, et al. Understanding the insight mechanism of chemical-mechanical degradation of layered Co-free Ni-rich cathode materials: a review. *Small* 2023;19:e2302208. DOI
5. Li W, Erickson EM, Manthiram A. High-nickel layered oxide cathodes for lithium-based automotive batteries. *Nat Energy* 2020;5:26-34. DOI
6. Deng T, Fan X, Cao L, et al. Designing in-situ-formed interphases enables highly reversible cobalt-free $LiNiO_2$ cathode for Li-ion and Li-metal batteries. *Joule* 2019;3:2550-64. DOI
7. Sun YK, Lee DJ, Lee YJ, Chen Z, Myung ST. Cobalt-free nickel rich layered oxide cathodes for lithium-ion batteries. *ACS Appl Mater Interfaces* 2013;5:11434-40. DOI PubMed
8. Li W, Lee S, Manthiram A. High-nickel NMA: a cobalt-free alternative to NMC and NCA cathodes for lithium-ion batteries. *Adv Mater* 2020;32:e2002718. DOI
9. Park G, Namkoong B, Kim S, Liu J, Yoon CS, Sun Y. Introducing high-valence elements into cobalt-free layered cathodes for practical lithium-ion batteries. *Nat Energy* 2022;7:946-54. DOI
10. Park N, Kim S, Kim M, et al. Mechanism of doping with high-valence elements for developing Ni-rich cathode materials. *Adv Energy Mater* 2023;13:2301530. DOI
11. Yoon CS, Jun D, Myung S, Sun Y. Structural stability of $LiNiO_2$ cycled above 4.2 V. *ACS Energy Lett* 2017;2:1150-5. DOI
12. Kim Y, Kim H, Manthiram A. A kinetic study on cobalt-free high-nickel layered oxide cathode materials for practical lithium-ion batteries. *J Power Sources* 2023;558:232633. DOI
13. Mesnier A, Manthiram A. Synthesis of $LiNiO_2$ at moderate oxygen pressure and long-term cyclability in lithium-ion full cells. *ACS Appl Mater Interfaces* 2020;12:52826-35. DOI PubMed
14. Wang X, Zhang B, Xiao Z, et al. Enhanced rate capability and mitigated capacity decay of ultrahigh-nickel cobalt-free $LiNi_{0.9}Mn_{0.1}O_2$ cathode at high-voltage by selective tungsten substitution. *Chin Chem Lett* 2023;34:107772. DOI
15. Kim JM, Xu Y, Engelhard MH, et al. Facile dual-protection layer and advanced electrolyte enhancing performances of cobalt-free/nickel-rich cathodes in lithium-ion batteries. *ACS Appl Mater Interfaces* 2022;14:17405-14. DOI
16. Yi M, Dolocan A, Manthiram A. Stabilizing the interphase in cobalt-free, ultrahigh-nickel cathodes for lithium-ion batteries. *Adv Funct Mater* 2023;33:2213164. DOI
17. Ryu H, Park G, Yoon CS, Sun Y. Suppressing detrimental phase transitions *via* tungsten doping of $LiNiO_2$ cathode for next-generation lithium-ion batteries. *J Mater Chem A* 2019;7:18580-8. DOI
18. Zhang Y, Li H, Liu J, Liu J, Ma H, Cheng F. Enhancing $LiNiO_2$ cathode materials by concentration-gradient yttrium modification for rechargeable lithium-ion batteries. *J Energy Chem* 2021;63:312-9. DOI
19. Yoon CS, Kim U, Park G, et al. Self-passivation of a $LiNiO_2$ cathode for a lithium-ion battery through Zr doping. *ACS Energy Lett* 2018;3:1634-9. DOI
20. Luo Y, Wei H, Tang L, et al. Nickel-rich and cobalt-free layered oxide cathode materials for lithium ion batteries. *Energy Stor Mater* 2022;50:274-307. DOI
21. Wang T, Yang J, Wang H, et al. Promoting reversibility of Co-free layered cathodes by Al and cation vacancy. *Adv Energy Mater* 2023;13:2204241. DOI
22. Seong WM, Manthiram A. Complementary effects of Mg and Cu incorporation in stabilizing the cobalt-free $LiNiO_2$ cathode for lithium-ion batteries. *ACS Appl Mater Interfaces* 2020;12:43653-64. DOI PubMed
23. Cui Z, Guo Z, Manthiram A. Assessing the intrinsic roles of key dopant elements in high-nickel layered oxide cathodes in lithium-based batteries. *Adv Energy Mater* 2023;13:2203853. DOI
24. Divakaran AM, Minakshi M, Bahri PA, et al. Rational design on materials for developing next generation lithium-ion secondary battery. *Prog Solid State Chem* 2021;62:100298. DOI
25. Li M, Lu J. Cobalt in lithium-ion batteries. *Science* 2020;367:979-80. DOI
26. Zheng J, Teng G, Xin C, et al. Role of superexchange interaction on tuning of Ni/Li disordering in layered $Li(Ni_xMn_yCo_z)O_2$. *J Phys Chem Lett* 2017;8:5537-42. DOI
27. Li H, Cormier M, Zhang N, Inglis J, Li J, Dahn JR. Is cobalt needed in Ni-rich positive electrode materials for lithium ion batteries? *J Electrochem Soc* 2019;166:A429-39. DOI
28. Liu T, Yu L, Liu J, et al. Understanding Co roles towards developing Co-free Ni-rich cathodes for rechargeable batteries. *Nat Energy* 2021;6:277-86. DOI
29. Tian R, Yin S, Zhang H, Song D, Ma Y, Zhang L. Influence of Al doping on the structure and electrochemical performance of the Co-free $LiNi_{0.8}Mn_{0.2}O_2$ cathode material. *Dalton Trans* 2023;52:11716-24. DOI
30. Shen L, Du F, Zhou Q, et al. Cobalt-free nickel-rich cathode materials based on Al/Mg co-doping of $LiNiO_2$ for lithium ion battery. *J Colloid Interface Sci* 2023;638:281-90. DOI

31. Park G, Sun HH, Noh T, et al. Nanostructured Co-free layered oxide cathode that affords fast-charging lithium-ion batteries for electric vehicles. *Adv Energy Mater* 2022;12:2202719. DOI
32. Zhong Q, von Sacken U. Crystal structures and electrochemical properties of $LiAl_yNi_{1-y}O_2$ solid solution. *J Power Sources* 1995;54:221-3. DOI
33. Nishida Y, Nakane K, Satoh T. Synthesis and properties of gallium-doped $LiNiO_2$ as the cathode material for lithium secondary batteries. *J Power Sources* 1997;68:561-4. DOI
34. Lin S, Fung K, Hon Y, Hon M. Crystallization kinetics and mechanism of the $Li_xNi_{2-x}O_2$ ($0 < x \leq 1$) from Li_2CO_3 and NiO. *J Crystal Growth* 2002;234:176-83. DOI
35. Croguennec L, Suard E, Willmann P, Delmas C. Structural and electrochemical characterization of the $LiNi_{1-y}Ti_yO_2$ electrode materials obtained by direct solid-state reactions. *Chem Mater* 2002;14:2149-57. DOI
36. Kong X, Li D, Fedorovskaya EO, Kallio T, Ren X. New insights in Al-doping effects on the $LiNiO_2$ positive electrode material by a sol-gel method. *Int J Energy Res* 2021;45:10489-99. DOI
37. van Bommel A, Dahn JR. Analysis of the growth mechanism of coprecipitated spherical and dense nickel, manganese, and cobalt-containing hydroxides in the presence of aqueous ammonia. *Chem Mater* 2009;21:1500-3. DOI
38. Kong X, Li D, Lahtinen K, Kallio T, Ren X. Effect of copper-doping on $LiNiO_2$ positive electrode for lithium-ion batteries. *J Electrochem Soc* 2020;167:140545. DOI
39. Ji H, Ben L, Yu H, Qiao R, Zhao W, Huang X. Electrolyzed $Ni(OH)_2$ precursor sintered with $LiOH/LiNiO_3$ mixed salt for structurally and electrochemically stable cobalt-free $LiNiO_2$ cathode materials. *ACS Appl Mater Interfaces* 2021;13:50965-74. DOI PubMed
40. Essehli R, Parejiya A, Muralidharan N, et al. Hydrothermal synthesis of Co-free NMA cathodes for high performance Li-ion batteries. *J Power Sources* 2022;545:231938. DOI
41. Cui Z, Xie Q, Manthiram A. A cobalt- and manganese-free high-nickel layered oxide cathode for long-life, safer lithium-ion batteries. *Adv Energy Mater* 2021;11:2102421. DOI
42. Zheng J, Ye Y, Liu T, et al. Ni/Li disordering in layered transition metal oxide: electrochemical impact, origin, and control. *ACC Chem Res* 2019;52:2201-9. DOI
43. Tan X, Peng W, Luo G, et al. Chemical and structural evolution during solid-state synthesis of cobalt-free nickel-rich layered oxide cathode. *Mater Today Energy* 2022;29:101114. DOI
44. Yu L, Zhao H, Sun J, Han Q, Zhu J, Lu J. Insights into micromorphological effects of cation disordering on Co-free layered oxide cathodes. *Adv Funct Mater* 2022;32:2204931. DOI
45. Su L, Jarvis K, Charalambous H, Dolocan A, Manthiram A. Stabilizing high-nickel cathodes with high-voltage electrolytes. *Adv Funct Mater* 2023;33:2213675. DOI
46. Cui Z, Manthiram A. Thermal stability and outgassing behaviors of high-nickel cathodes in lithium-ion batteries. *Angew Chem Int Ed* 2023;62:e202307243. DOI PubMed
47. Rougier A, Saadoune I, Gravereau P, Willmann P, Delmasa C. Effect of cobalt substitution on cationic distribution in $LiNi_{1-y}Co_yO_2$ electrode materials. *Solid State Ion* 1996;90:83-90. DOI
48. Wei H, Tang L, Huang Y, et al. Comprehensive understanding of Li/Ni intermixing in layered transition metal oxides. *Mater Today* 2021;51:365-92. DOI
49. Kanamori J. Superexchange interaction and symmetry properties of electron orbitals. *J Phys Chem Solids* 1959;10:87-98. DOI
50. Xiao Y, Liu T, Liu J, et al. Insight into the origin of lithium/nickel ions exchange in layered $Li(Ni_xMn_yCo_z)O_2$ cathode materials. *Nano Energy* 2018;49:77-85. DOI
51. Wang D, Xin C, Zhang M, et al. Intrinsic role of cationic substitution in tuning Li/Ni mixing in high-Ni layered oxides. *Chem Mater* 2019;31:2731-40. DOI
52. Kim Y, Kim D, Kang S. Experimental and first-principles thermodynamic study of the formation and effects of vacancies in layered lithium nickel cobalt oxides. *Chem Mater* 2011;23:5388-97. DOI
53. Reed J, Ceder G. Role of electronic structure in the susceptibility of metastable transition-metal oxide structures to transformation. *Chem Rev* 2004;104:4513-33. DOI PubMed
54. Yu H, Qian Y, Otani M, et al. Study of the lithium/nickel ions exchange in the layered $LiNi_{0.42}Mn_{0.42}Co_{0.16}O_2$ cathode material for lithium ion batteries: experimental and first-principles calculations. *Energy Environ Sci* 2014;7:1068-78. DOI
55. Wang C, Han L, Zhang R, et al. Resolving atomic-scale phase transformation and oxygen loss mechanism in ultrahigh-nickel layered cathodes for cobalt-free lithium-ion batteries. *Matter* 2021;4:2013-26. DOI
56. Ahmed S, Bianchini M, Pokle A, et al. Visualization of light elements using 4D STEM: the layered-to-rock salt phase transition in $LiNiO_2$ cathode material. *Adv Energy Mater* 2020;10:2001026. DOI
57. Cheng J, Ouyang B, Persson KA. Mitigating the High-charge detrimental phase transformation in $LiNiO_2$ using doping engineering. *ACS Energy Lett* 2023;8:2401-7. DOI
58. Kong F, Liang C, Wang L, et al. Kinetic stability of bulk $LiNiO_2$ and surface degradation by oxygen evolution in $LiNiO_2$-based cathode materials. *Adv Energy Mater* 2019;9:1802586. DOI
59. Wang L, Maxisch T, Ceder G. A First-principles approach to studying the thermal stability of oxide cathode materials. *Chem Mater* 2007;19:543-52. DOI
60. Li L, Yu J, Darbar D, et al. Atomic-scale mechanisms of enhanced electrochemical properties of Mo-doped Co-free layered oxide cathodes for lithium-ion batteries. *ACS Energy Lett* 2019;4:2540-6. DOI

61. Li H, Hua W, Liu-théato X, et al. New insights into lithium hopping and ordering in $LiNiO_2$ cathodes during Li (De)intercalation. *Chem Mater* 2021;33:9546-59. DOI
62. Ikeda N, Konuma I, Rajendra HB, Aida T, Yabuuchi N. Why is the O3 to O1 phase transition hindered in $LiNiO_2$ on full delithiation? *J Mater Chem A* 2021;9:15963-7. DOI
63. de Biasi L, Schiele A, Roca-Ayats M, et al. Phase transformation behavior and stability of $LiNiO_2$ cathode material for Li-ion batteries obtained from in situ gas analysis and operando X-Ray diffraction. *ChemSusChem* 2019;12:2240-50. DOI
64. Zhang SS. Problems and their origins of Ni-rich layered oxide cathode materials. *Energy Stor Mater* 2020;24:247-54. DOI
65. Bi Y, Li Q, Yi R, Xiao J. To pave the way for large-scale electrode processing of moisture-sensitive Ni-rich cathodes. *J Electrochem Soc* 2022;169:020521. DOI
66. Marchand-brynaert J, Jongen N, Dewez J. Surface hydroxylation of poly(vinylidene fluoride) (PVDF) film. *J Polym Sci A Polym Chem* 1997;35:1227-35. DOI
67. Dai P, Kong X, Yang H, Li J, Zeng J, Zhao J. Single-crystal Ni-rich layered $LiNi_{0.9}Mn_{0.1}O_2$ enables superior performance of Co-free cathodes for lithium-ion batteries. *ACS Sustain Chem Eng* 2022;10:4381-90. DOI
68. Kaneda H, Furuichi Y, Ikezawa A, Arai H. Single-crystal-like durable $LiNiO_2$ positive electrode materials for lithium-ion batteries. *ACS Appl Mater Interfaces* 2022;14:52766-78. DOI PubMed
69. Luu NS, Meza PE, Tayamen AM, et al. Enabling ambient stability of $LiNiO_2$ lithium-ion battery cathode materials via graphene-cellulose composite coatings. *Chem Mater* 2023;35:5150-9. DOI
70. Ober S, Mesnier A, Manthiram A. Surface stabilization of cobalt-free $LiNiO_2$ with niobium for lithium-ion batteries. *ACS Appl Mater Interfaces* 2023;15:1442-51. DOI PubMed
71. Kim Y, Kim H, Shin W, Jo E, Manthiram A. Insights into the microstructural engineering of cobalt-free, high-nickel cathodes based on surface energy for lithium-ion batteries. *Adv Energy Mater* 2023;13:2204054. DOI
72. Mu L, Kan WH, Kuai C, et al. Structural and electrochemical impacts of Mg/Mn dual dopants on the $LiNiO_2$ cathode in Li-metal batteries. *ACS Appl Mater Interfaces* 2020;12:12874-82. DOI
73. Chu Y, Zhou J, Liu W, Chu F, Li J, Wu F. Cobalt-free $LiNiO_2$ with a selenium coating as a high-energy layered cathode material for lithium-ion batteries. *Small Sci* 2023;3:2300023. DOI
74. Zaker N, Geng C, Rathore D, et al. Probing the mysterious behavior of tungsten as a dopant inside pristine cobalt-free nickel-rich cathode materials. *Adv Funct Mater* 2023;33:2211178. DOI
75. Liu L, Zhao Y, Jiang G, et al. Dual-site lattice co-doping strategy regulated crystal-structure and microstructure for enhanced cycling stability of Co-free Ni-rich layered cathode. *Nano Res* 2023;16:9250-8. DOI
76. Hu C, Ma J, Li A, et al. Structural reinforcement through high-valence Nb doping to boost the cycling stability of Co-free and Ni-rich $LiNi_{0.9}Mn_{0.1}O_2$ cathode materials. *Energy Fuels* 2023;37:8005-13. DOI
77. Cao H, Du F, Adkins J, et al. Al-doping induced superior lithium ion storage capability of $LiNiO_2$ spheres. *Ceram Int* 2020;46:20050-60. DOI
78. Xu T, Du F, Wu L, Fan Z, Shen L, Zheng J. Boosting the electrochemical performance of $LiNiO_2$ by extra low content of Mn-doping and its mechanism. *Electrochim Acta* 2022;417:140345. DOI
79. Sathiyamoorthi R, Shakkthivel P, Ramalakshmi S, Shul Y. Influence of Mg doping on the performance of $LiNiO_2$ matrix ceramic nanoparticles in high-voltage lithium-ion cells. *J Power Sources* 2007;171:922-7. DOI
80. Geng C, Rathore D, Heino D, et al. Mechanism of action of the tungsten dopant in $LiNiO_2$ positive electrode materials. *Adv Energy Mater* 2022;12:2103067. DOI
81. Yang Z, Mu L, Hou D, et al. Probing dopant redistribution, phase propagation, and local chemical changes in the synthesis of layered oxide battery cathodes. *Adv Energy Mater* 2021;11:2002719. DOI
82. Hua W, Zhang J, Wang S, et al. Long-range cationic disordering induces two distinct degradation pathways in Co-free Ni-rich layered cathodes. *Angew Chem Int Ed* 2023;62:e202214880. DOI
83. Mu L, Yang Z, Tao L, et al. The sensitive surface chemistry of Co-free, Ni-rich layered oxides: identifying experimental conditions that influence characterization results. *J Mater Chem A* 2020;8:17487-97. DOI
84. Kong F, Liang C, Longo RC, et al. Conflicting roles of anion doping on the electrochemical performance of Li-ion battery cathode materials. *Chem Mater* 2016;28:6942-52. DOI
85. Pouillerie C, Croguennec L, Biensan P, Willmann P, Delmas C. Synthesis and characterization of new $LiNi_{1-y}Mg_yO_2$ positive electrode materials for lithium-ion batteries. *J Electrochem Soc* 2000;147:2061. DOI
86. Liu A, Zhang N, Stark JE, Arab P, Li H, Dahn JR. Synthesis of Co-free Ni-rich single crystal positive electrode materials for lithium ion batteries: part I. two-step lithiation method for Al- or Mg-doped $LiNiO_2$. *J Electrochem Soc* 2021;168:040531. DOI
87. Liu Q, Wu Z, Sun J, et al. Facile synthesis of crack-free single-crystalline Al-doped Co-free Ni-rich cathode material for lithium-ion batteries. *Electrochim Acta* 2023;437:141473. DOI
88. Nie L, Wang Z, Zhao X, et al. Cation/anion codoped and cobalt-free Li-rich layered cathode for high-performance Li-ion batteries. *Nano Lett* 2021;21:8370-7. DOI
89. Xi Y, Wang M, Xu L, et al. A new Co-free Ni-rich $LiNi_{0.8}Fe_{0.1}Mn_{0.1}O_2$ cathode for low-cost Li-ion batteries. *ACS Appl Mater Interfaces* 2021;13:57341-9. DOI
90. Deng S, Li Y, Dai Q, et al. Structure and primary particle double-tuning by trace nano-TiO_2 for a high-performance $LiNiO_2$ cathode material. *Sustain Energy Fuels* 2019;3:3234-43. DOI

91. Yoon CS, Choi M, Jun D, et al. Cation ordering of Zr-doped $LiNiO_2$ cathode for lithium-ion batteries. *Chem Mater* 2018;30:1808-14. DOI
92. Tatsumi K, Sasano Y, Muto S, et al. Local atomic and electronic structures around Mg and Al dopants in $LiNiO_2$ electrodes studied by XANES and ELNES and first-principles calculations. *Phys Rev B* 2008;78:045108. DOI
93. Liu A, Zhang N, Stark JE, Arab P, Li H, Dahn JR. Synthesis of Co-free Ni-rich single crystal positive electrode materials for lithium ion batteries: part II. one-step lithiation method of Mg-doped $LiNiO_2$. *J Electrochem Soc* 2021;168:050506. DOI
94. Weber R, Li H, Chen W, Kim C, Plucknett K, Dahn JR. In situ XRD studies during synthesis of single-crystal $LiNiO_2$, $LiNi_{0.975}Mg_{0.025}O_2$, and $LiNi_{0.95}Al_{0.05}O_2$ cathode materials. *J Electrochem Soc* 2020;167:100501. DOI
95. Laine P, Välikangas J, Kauppinen T, et al. Synergistic effects of low - level magnesium and chromium doping on the electrochemical performance of $LiNiO_2$ cathodes. *J Solid State Electrochem* 2024;28:85-101. DOI
96. Mu L, Zhang R, Kan WH, et al. Dopant distribution in Co-free high-energy layered cathode materials. *Chem Mater* 2019;31:9769-76. DOI
97. Min K, Seo SW, Song YY, Lee HS, Cho E. A first-principles study of the preventive effects of Al and Mg doping on the degradation in $LiNi_{0.8}Co_{0.1}Mn_{0.1}O_2$ cathode materials. *Phys Chem Chem Phys* 2017;19:1762-9. DOI
98. Fang L, Wang M, Zhou Q, Xu H, Hu W, Li H. Suppressing cation mixing and improving stability by F doping in cathode material $LiNiO_2$ for Li-ion batteries: first-principles study. *Colloid Surface A* 2020;600:124940. DOI
99. Li B, Yan H, Ma J, et al. Manipulating the electronic structure of Li-rich manganese-based oxide using polyanions: towards better electrochemical performance. *Adv Funct Mater* 2014;24:5112-8. DOI
100. Kang J, Han B. First-principles study on the thermal stability of $LiNiO_2$ materials coated by amorphous Al_2O_3 with atomic layer thickness. *ACS Appl Mater Interfaces* 2015;7:11599-603. DOI
101. Woo JH, Trevey JE, Cavanagh AS, et al. Nanoscale interface modification of $LiCoO_2$ by Al_2O_3 atomic layer deposition for solid-state Li batteries. *J Electrochem Soc* 2012;159:A1120-4. DOI
102. Scott ID, Jung YS, Cavanagh AS, et al. Ultrathin coatings on nano-$LiCoO_2$ for Li-ion vehicular applications. *Nano Lett* 2011;11:414-8. DOI
103. Riley LA, Van Atta S, Cavanagh AS, et al. Electrochemical effects of ALD surface modification on combustion synthesized $LiNi_{1/3}Mn_{1/3}Co_{1/3}O_2$ as a layered-cathode material. *J Power Sources* 2011;196:3317-24. DOI
104. Zhang X, Belharouak I, Li L, et al. Structural and electrochemical study of Al_2O_3 and TiO_2 coated $Li_{1.2}Ni_{0.13}Mn_{0.54}Co_{0.13}O_2$ cathode material using ALD. *Adv Energy Mater* 2013;3:1299-307. DOI
105. Seok Jung Y, Cavanagh AS, Yan Y, George SM, Manthiram A. Effects of atomic layer deposition of Al_2O_3 on the $Li[Li_{0.20}Mn_{0.54}Ni_{0.13}Co_{0.13}]O_2$ cathode for lithium-ion batteries. *J Electrochem Soc* 2011;158:A1298. DOI
106. Brow R, Donakowski A, Mesnier A, et al. Mechanical pulverization of Co-free nickel-rich cathodes for improved high-voltage cycling of lithium-ion batteries. *ACS Appl Energy Mater* 2022;5:6996-7005. DOI
107. Hou A, Xu S, Xu K, Zhang M, Zhao D. Comparative studies of tungsten and zirconium doping on single crystal cobalt-free cathode material. *Ionics* 2021;27:4241-8. DOI
108. Cheng J, Mu L, Wang C, et al. Enhancing surface oxygen retention through theory-guided doping selection in $Li_{1-x}NiO_2$ for next-generation lithium-ion batteries. *J Mater Chem A* 2020;8:23293-303. DOI
109. Huang G, Wang R, Lv X, et al. Effect of niobium doping on structural stability and electrochemical properties of $LiNiO_2$ cathode for Li-ion batteries. *J Electrochem Soc* 2022;169:040533. DOI
110. Li J, Zhou Z, Luo Z, et al. Microcrack generation and modification of Ni-rich cathodes for Li-ion batteries: a review. *Sustain Mater Technol* 2021;29:e00305. DOI
111. Jamil S, Yu R, Wang Q, et al. Enhanced cycling stability of nickel-rich layered oxide by tantalum doping. *J Power Sources* 2020;473:228597. DOI
112. Jeong M, Kim H, Lee W, Ahn S, Lee E, Yoon W. Stabilizing effects of Al-doping on Ni-rich $LiNi_{0.80}Co_{0.15}Mn_{0.05}O_2$ cathode for Li rechargeable batteries. *J Power Sources* 2020;474:228592. DOI
113. Kim U, Kim J, Hwang J, Ryu H, Yoon CS, Sun Y. Compositionally and structurally redesigned high-energy Ni-rich layered cathode for next-generation lithium batteries. *Mater Today* 2019;23:26-36. DOI
114. Kim U, Park J, Aishova A, et al. Microstructure engineered Ni-rich layered cathode for electric vehicle batteries. *Adv Energy Mater* 2021;11:2100884. DOI
115. Uzun D, Doğrusöz M, Mazman M, et al. Effect of MnO_2 coating on layered $Li(Li_{0.1}Ni_{0.3}Mn_{0.5}Fe_{0.1})O_2$ cathode material for Li-ion batteries. *Solid State Ion* 2013;249-50:171-6. DOI
116. Qian G, Zhang Y, Li L, et al. Single-crystal nickel-rich layered-oxide battery cathode materials: synthesis, electrochemistry, and intra-granular fracture. *Energy Stor Mater* 2020;27:140-9. DOI
117. Zhu J, Zheng J, Cao G, et al. Flux-free synthesis of single-crystal $LiNi_{0.8}Co_{0.1}Mn_{0.1}O_2$ boosts its electrochemical performance in lithium batteries. *J Power Sources* 2020;464:228207. DOI
118. Liu J, Yuan Y, Zheng J, et al. Understanding the synthesis kinetics of single-crystal Co-free Ni-rich cathodes. *Angew Chem Int Ed* 2023;62:e202302547. DOI
119. Mesnier A, Manthiram A. Heuristics for molten-salt synthesis of single-crystalline ultrahigh-nickel layered oxide cathodes. *ACS Appl Mater Interfaces* 2023;15:12895-907. DOI PubMed
120. Shen J, Zhang B, Huang W, et al. Achieving thermodynamic stability of single-crystal Co-free Ni-rich cathode material for high

voltage lithium-ion batteries. *Adv Funct Mater* 2023;33:2300081. DOI

121. Xia Y, Chen A, Wang K, et al. Binary-compositional core-shell structure Ni-rich cathode material with radially oriented primary particles in shell for long cycling lifespan lithium-ion batteries. *Mater Today Energy* 2023;34:101292. DOI
122. Song L, Jiang P, Xiao Z, et al. Core-shell structure $LiNi_{0.8}Co_{0.1}Mn_{0.1}O_2$ cathode material with improved electrochemical performance at high voltage. *Ionics* 2021;27:949-59. DOI
123. Mallick S, Patel A, Sun X, et al. Low-cobalt active cathode materials for high-performance lithium-ion batteries: synthesis and performance enhancement methods. *J Mater Chem A* 2023;11:3789-821. DOI
124. Zhang S, Gao P, Wang Y, Li J, Zhu Y. Cobalt-free concentration-gradient $Li[Ni_{0.9}Mn_{0.1}]O_2$ cathode material for lithium-ion batteries. *J Alloy Compd* 2021;885:161005. DOI
125. Jeong D, Kwon D, Kim HJ, Shim J. Striking a balance: exploring optimal functionalities and composition of highly adhesive and dispersing binders for high-nickel cathodes in lithium-ion batteries. *Adv Energy Mater* 2023;13:2302845. DOI
126. Pham HQ, Kim G, Jung HM, Song S. Fluorinated polyimide as a novel high-voltage binder for high-capacity cathode of lithium-ion batteries. *Adv Funct Mater* 2018;28:1704690. DOI
127. Chang B, Kim J, Cho Y, et al. Highly elastic binder for improved cyclability of nickel-rich layered cathode materials in lithium-ion batteries. *Adv Energy Mater* 2020;10:2001069. DOI
128. Das D, Manna S, Puravankara S. Electrolytes, Additives and binders for NMC cathodes in Li-ion batteries - a review. *Batteries* 2023;9:193. DOI